



Sources, transport
and deposition of
iron in the global
atmosphere

R. Wang et al.

Sources, transport and deposition of iron in the global atmosphere

R. Wang^{1,2,3}, Y. Balkanski^{1,3}, O. Boucher⁴, L. Bopp¹, A. Chappell⁵, P. Ciais^{1,3},
D. Hauglustaine¹, J. Peñuelas^{6,7}, and S. Tao^{2,3}

¹Laboratoire des Sciences du Climat et de l'Environnement, CEA CNRS UVSQ,
Gif-sur-Yvette, France

²Laboratory for Earth Surface Processes, College of Urban and Environmental Sciences,
Peking University, Beijing, China

³Sino-French Institute for Earth System Science, College of Urban and Environmental
Sciences, Peking University, Beijing, China

⁴Laboratoire de Météorologie Dynamique, IPSL/CNRS, Université Pierre et Marie Curie,
France

⁵CSIRO Land & Water National Research Flagship, GPO Box 1666, Canberra, ACT 2601,
Australia

⁶Consejo Superior de Investigaciones Científicas, Global Ecology Unit CREAM-CEAB-UAB,
Spain

⁷Centre de Recerca Ecològica i Aplicacions Forestals, Spain

Title Page

Abstract

Introduction

Conclusions

References

Tables

Figures



Back

Close

Full Screen / Esc

Printer-friendly Version

Interactive Discussion



Received: 30 December 2014 – Accepted: 25 February 2015 – Published: 12 March 2015

Correspondence to: R. Wang (rong.wang@lsce.ipsl.fr)

Published by Copernicus Publications on behalf of the European Geosciences Union.

ACPD

15, 7645–7705, 2015

Sources, transport and deposition of iron in the global atmosphere

R. Wang et al.

Title Page

Abstract

Introduction

Conclusions

References

Tables

Figures



Back

Close

Full Screen / Esc

Printer-friendly Version

Interactive Discussion



Abstract

Atmospheric deposition of iron (Fe) plays an important role in controlling oceanic primary productivity. However, the sources of Fe in the atmosphere are not well understood. In particular, the combustion sources of Fe and their deposition over oceans are not accounted for in current biogeochemical models of the carbon cycle. Here we used a mass-balance method to estimate the emissions of Fe from the combustion of fossil fuels and biomass by accounting for the Fe contents in fuel and the partitioning of Fe during combustion. The emissions of Fe attached to aerosols from combustion sources were estimated by particle size, and their uncertainties were quantified by a Monte Carlo simulation. The emissions of Fe from mineral sources were estimated using the latest soil mineralogical database to date. As a result, the total Fe emissions from combustion averaged for 1960–2007 were estimated to be 5.1 Tgyr^{-1} (90% confidence of 2.2 to 11.5). Of these emissions, 2, 33 and 65% were emitted in particles $<1 \mu\text{m}$ (PM_1), $1\text{--}10 \mu\text{m}$ (PM_{1-10}), and $>10 \mu\text{m}$ ($\text{PM}_{>10}$), respectively, compared to total Fe emissions from mineral sources of 41.0 Tgyr^{-1} . For combustion sources, different temporal trends were found in fine and medium-to-coarse particles, with a notable increase in Fe emissions in PM_1 and PM_{1-10} since 2000 due to a rapid increase from motor vehicles. These emissions have been introduced in a global 3-D transport model run at a spatial resolution of 0.94° latitude by 1.28° longitude to evaluate our estimation of Fe emissions. The modelled Fe concentrations were compared to measurements at 825 sampling stations. The deviation between modelled and observed Fe concentrations attached to aerosols at the surface was within a factor of two at most sampling stations, and the deviation was within a factor of 1.5 at sampling stations dominated by combustion sources. We analyzed the relative contribution of combustion sources to total Fe concentrations over different regions of the world. The new mineralogical database led to a modest improvement in the simulation relative to station data even in dust dominated regions, but could provide useful information on the chemical forms of Fe in dust for coupling with ocean biota models. We estimated a total Fe deposition

Sources, transport and deposition of iron in the global atmosphere

R. Wang et al.

Title Page

Abstract

Introduction

Conclusions

References

Tables

Figures



Back

Close

Full Screen / Esc

Printer-friendly Version

Interactive Discussion



sink of 8.4 Tgyr^{-1} over global oceans, 6.6 % of which originated from the combustion sources. The higher than previously estimated combustion-related Fe emissions implies a larger atmospheric input of soluble Fe over the northern Atlantic and northern Pacific Oceans, which is expected to enhance the biological carbon pump in those regions.

1 Introduction

Sea-water dissolved iron (Fe) concentration is a primary factor that limits or co-limits the growth of phytoplankton in large regions of the global oceans (Martin et al., 1991; Moore et al., 2013). As such, Fe availability influences the transfer and sequestration of carbon into the deep ocean (Boyd et al., 2000; Moore et al., 2004). Both ice-core and marine-sediment records indicate high rates of aeolian dust and hence Fe supply to the oceans at the Last Glacial Maximum, implying a potential link between Fe availability, marine productivity, atmospheric CO_2 and climate through Fe fertilization (Martin, 1990; Ridgwell and Watson, 2002). Over the Industrial Era, the increase of Fe deposition in dust was estimated to be responsible for a decrease of atmospheric CO_2 by 4 ppm (Mahowald et al., 2011), with a large uncertainty.

Atmospheric deposition provides an important source of Fe to the marine biota (Martin, 1990; Duce and Tindale, 1991; Johnson et al., 1997; Fung et al., 2000; Gao et al., 2001; Conway and John, 2014). Early studies of the effects of Fe fertilization, however, mostly focused on aeolian dust sources (Hand et al., 2004; Luo et al., 2003; Gregg et al., 2003; Moore et al., 2004; Mahowald et al., 2005; Fan et al., 2006). Observed concentrations of soluble Fe were not properly captured by the models simulating the atmospheric transport, chemical processing and deposition of Fe in aerosols (Hand et al., 2004; Luo et al., 2005; Fan et al., 2006), thus suggesting the existence of other sources. Guieu et al. (2005) proposed that the burning of biomass could be an additional source of soluble Fe in the Ligurian Sea. Chuang et al. (2005) reported that soluble Fe observed at an atmospheric deposition measurement station in Korea was not

Sources, transport and deposition of iron in the global atmosphere

R. Wang et al.

Title Page

Abstract

Introduction

Conclusions

References

Tables

Figures



Back

Close

Full Screen / Esc

Printer-friendly Version

Interactive Discussion



dominated by mineral sources, even during dust storms. Sedwick et al. (2007) hypothesized that the anthropogenic emissions of Fe from combustion could play a significant role in the atmospheric input of bioavailable Fe to the surface of the Atlantic Ocean.

The first estimate of Fe emissions from fossil fuels and biomass burning reported a total Fe emission of 1.7 Tgyr^{-1} (Luo et al., 2008). Ito and Feng (2010) subsequently obtained a lower estimate of 1.2 Tgyr^{-1} . By prescribing a high emission factor of Fe from ships, Ito (2013) later derived a total Fe emission of 1.7 Tgyr^{-1} and suggested a large contribution by shipping to the deposition of soluble Fe over the northern Pacific Ocean and the East China Sea. However, these authors suggested that more work was required to reduce the uncertainty in Fe emissions, particularly from the combustion of petroleum and biomass.

The mineral composition of dust is a key factor in the chemical forms of Fe, and it determines the solubility and thus the bioavailability of Fe. Nickovic et al. (2012) developed a global data set to represent the mineral composition of soil in arid and semi-arid areas. This mineralogical data set improved the agreement between simulated and measured concentrations of soluble Fe (Nickovic et al., 2013; Ito and Xu, 2014). More recently, Journet et al. (2014) developed a new data set of soil mineralogy (including soil Fe content) covering most dust source regions of the world at a resolution of $0.5^\circ \times 0.5^\circ$, with the aim to improve the modelling of the chemical forms of Fe in dust.

In this study, we estimated the emissions of Fe from combustion sources for 222 countries/territories over 1960 to 2007 period using a new method based on Fe content of fuel and Fe budget during combustion. We re-estimated Fe emissions from mineral sources based on the latest mineralogical database. Our estimates of Fe sources were evaluated by an atmospheric transport model at a fine resolution. The impact of the estimated combustion-related and mineral emissions of Fe on the model-data misfits at 825 stations measuring Fe concentration in surface aerosol and 30 stations measuring Fe deposition was investigated for different regions and stations.

Sources, transport and deposition of iron in the global atmosphere

R. Wang et al.

Title Page

Abstract

Introduction

Conclusions

References

Tables

Figures

◀

▶

◀

▶

Back

Close

Full Screen / Esc

Printer-friendly Version

Interactive Discussion



Database version 3) (van der Werf et al., 2010) for 1997–2007 and by RETRO (REanalysis of the TROpospheric chemical composition over the past 40 years) for 1960–1996 (Schulz et al., 2008). RETRO does not provide data for deforestation fires separately, so that the average fractions of deforestation fires in total forest fires by GFED3 were applied for 1960–1996.

2.5 Uncertainty of Fe emissions from combustion

A Monte Carlo ensemble simulation was run 1000 times by randomly varying parameters in the model, including fuel consumption, the Fe content, the fraction of Fe retained in the residue ash, the size distribution of Fe emission, the technology division of control device. Normal (petroleum, biodiesel, and dung cake) or log-normal (coal, grass, wood, and crop residues) distribution was adopted for the Fe content of fuel, as described above. The fraction of Fe retained in the residual ash was assumed to be uniformly distributed with ranges summarized in Sect. 2.3. Uncertainties in the fuel-consumption data and the technology divisions were quantified by prescribing a uniform distribution with a fixed relative standard deviation, as introduced in the previous studies (Wang et al., 2013, 2014a; Chen et al., 2013).

2.6 Emissions of Fe from mineral sources

We estimated the content of Fe in dust based on the largest mineralogical database to date (Journet et al., 2014). Journet et al. (2014) provided global $0.5^\circ \times 0.5^\circ$ maps for six types of Fe-containing minerals (illite, smectite, kaolinite, chlorite, vermiculite, and feldspars) and two types of Fe oxides (hematite and goethite) in the clay ($< 2.0\mu\text{m}$) and only goethite in the silt ($> 2.0\mu\text{m}$) fraction. A global $0.5^\circ \times 0.5^\circ$ map of Fe content in clay fraction was obtained (Fig. S2) by combining the Fe content of each mineral (Journet et al., 2008). The LMDz-INCA global model (Sect. 2.7) was run for 2000–2011 at a resolution of 0.94° latitude by 1.28° longitude to produce an averaged field of dust.

Title Page

Abstract

Introduction

Conclusions

References

Tables

Figures

◀

▶

◀

▶

Back

Close

Full Screen / Esc

Printer-friendly Version

Interactive Discussion



2.7 Modelling the atmospheric transport and deposition of Fe aerosols

We used the LMDz-INCA global chemistry-aerosol-climate model coupling on-line the LMDz (Laboratoire de Météorologie Dynamique, version 4) General Circulation Model (Hourdin et al., 2006) and the INCA (INteraction with Chemistry and Aerosols, version 4) model (Hauglustaine et al., 2004; Schulz, 2007; Balkanski, 2011) to simulate the atmospheric transport and distributions of Fe emitted from combustion and mineral sources. The interaction between the atmosphere and the land surface is ensured through the coupling of LMDz with the ORCHIDEE (ORganizing Carbon and Hydrology In Dynamic Ecosystems, version 9) dynamical vegetation model (Krinner et al., 2005). In the present configuration, the model was run at a horizontal resolution of 0.94° latitude by 1.28° longitude with 39 vertical layers from the surface to 80 km. In all simulations, meteorological data from the European Centre for Medium-Range Weather Forecasts (ECMWF) reanalysis have been used. The relaxation of the GCM winds towards ECMWF meteorology was performed by applying at each time step a correction term to the GCM predicted u and v wind components with a relaxation time of 6 h (Hourdin and Issartel, 2000; Hauglustaine et al., 2004). The ECMWF fields are provided every 6 h and interpolated onto the LMDz grid.

In the model, the emissions of dust were calculated as a function of wind velocities at a height of 10 m (with a threshold value) and of the clay content from dust source locations (Schulz et al., 1998). The simulated concentrations and optical depths of dust have been validated by measurements (Schulz et al., 1998; Guelle et al., 2000; Balkanski et al., 2004, 2007). For transport, the model uses a computationally efficient scheme to represent the size distribution of dust. The tracer is treated as a log-normal distribution with a mass median diameter (MMD) and a fixed geometric σ (defined as the σ of log-transformed sizes). Hygroscopic growth and removal processes are assumed to affect the MMD rather than the width of the distribution (Schulz et al., 1998, 2007). After being emitted, dust with a MMD of $2.5\mu\text{m}$ and a geometric σ of

ACPD

15, 7645–7705, 2015

Sources, transport and deposition of iron in the global atmosphere

R. Wang et al.

Title Page

Abstract

Introduction

Conclusions

References

Tables

Figures



Back

Close

Full Screen / Esc

Printer-friendly Version

Interactive Discussion



2.0 is transported and removed by sedimentation (Slinn and Slinn, 1980), wet and dry deposition (Balkanski et al., 2004, 2010, 2011).

The emitted Fe from combustion sources were partitioned into three size bins, with Fe in PM_1 as a fine mode (MMD = $0.34\ \mu\text{m}$, geometric $\sigma = 1.59$), Fe in PM_{1-10} as a coarse mode (MMD = $3.4\ \mu\text{m}$, geometric $\sigma = 2.0$), and Fe in $PM_{>10}$ as a super coarse mode (MMD = $34\ \mu\text{m}$, geometric $\sigma = 2.$) (Mamane et al., 1986; Querol et al., 1995; Valmari et al., 1999). Sedimentation, dry and wet deposition accounted for the Fe in PM_{1-10} and $PM_{>10}$, as for dust, and the Fe in PM_1 as for BC (Balkanski et al., 2004, 2010, 2011). Approximately 25% of the Fe in fine particles (diameter $< 0.61\ \mu\text{m}$) is bound to organic matter and thus insoluble (Espinosa et al., 2002), so we assumed that 25% of the Fe in PM_1 was simulated as hydrophobic and not subject to in-cloud scavenging, while the remainder was treated as hydrophilic BC. We did not account for the conversion from hydrophobic to hydrophilic Fe in the atmospheric transport, and the ratio between the two phases varied due to their different removal rates in the atmosphere.

A total of eight simulations were run for a typical year (2005) for the Fe emitted from the combustion of coal (three size classes), petroleum (two size classes), and biomass (three size classes). The gridded Fe emissions from combustion as monthly means averaged over 1990–2007 were used as an input to the model. Between 1990 and 2007, the modelled Fe concentrations attached to aerosols in the surface layer of the atmosphere at a measurement station was derived by scaling the modelled Fe concentrations for year 2005 by the ratio of the national Fe emission in the year to the 1990–2007 average in the country.

Sources, transport and deposition of iron in the global atmosphere

R. Wang et al.

Title Page

Abstract

Introduction

Conclusions

References

Tables

Figures



Back

Close

Full Screen / Esc

Printer-friendly Version

Interactive Discussion



3 Emission sources of Fe

3.1 Emissions of Fe from combustion

Based on the fuel consumptions and Fe emission rates, the average global Fe emissions for 1960–2007 was 5.1 Tgyr^{-1} from combustion sources, with 0.041, 1.32, and 3.7 Tgyr^{-1} of Fe emitted in PM_1 , PM_{1-10} , and $\text{PM}_{>10}$, respectively. The Monte Carlo simulation of emission parameters shows that the Fe emissions were log-normally distributed (Fig. 1). The σ of \log_{10} -transformed Fe emissions ($\log_{10}\sigma$) was 0.22 for the global total, corresponding to a 90 % confidence range of 2.24 to 11.52 Tgyr^{-1} , or –56 to +127 % relative to the central estimate. In addition, the $\log_{10}\sigma$ varied from 0.09 to 0.27 for the emissions from different fuels (Fig. 1a). Due to a relatively large error in the Fe content of coal, the range of uncertainty of Fe emission from coal was larger than that of other fuels. Removing the variations of Fe content in fuel reduced the overall variation ($\log_{10}\sigma$) of Fe emissions by 66 % (coal), 34 % (petroleum) and 52 % (biomass). Consequently, a large contribution of uncertain Fe content in coal causes the range of uncertainty of Fe emissions in coarse particles to be larger than in fine particles (Fig. 1b).

The relative contributions of combustion sources to Fe emissions in different sizes are shown in Fig. 2. It shows that Fe emissions in medium-to-coarse particles (PM_{1-10} or $\text{PM}_{>10}$) are dominated by the combustion of coal in power plants and industry, followed by a notable contribution from the natural burning of biomass. By contrast, the combustion of petroleum (36 %), followed by coal (38 %) and biomass (26 %), contributed most to Fe emissions in fine particles (PM_1). The different source profiles are important for determining the Fe solubility and are discussed in Sect. 7. For example, the observed solubility of Fe might be primarily controlled by the particle size of dust (Baker and Jickells, 2006), but also varies in the fly ash from different fuels (Schroth et al., 2009; Bowie et al., 2009; Chen et al., 2012).

Title Page

Abstract

Introduction

Conclusions

References

Tables

Figures



Back

Close

Full Screen / Esc

Printer-friendly Version

Interactive Discussion



of Environmental Protection of the People's Republic of China, 2008) together led to a slowdown or even a reversal of the increase of Fe emissions in the region.

The temporal trends of Fe emissions of fine and medium-to-coarse particles also notably differed. Before 1985, Fe emissions of fine and medium-to-coarse particles both increased, due to a rapid increase in fuel consumptions. After 1985, Fe emissions of fine particles first decreased and re-increased after 2000, while Fe emissions of medium-to-coarse particles continuously decreased. Two explanations can account for the decoupling. First, the control devices equipped in industry can remove Fe in medium-to-coarse particles more effectively than fine particles (Yi et al., 2008). Second, the consumption of petroleum has been increasing in both developed and developing countries, sustaining fine-particle Fe emissions. In particular, Fe emission in fine particles in Asia had increased recently after a respite in the 1990s. The spatial distributions of Fe emissions from combustion sources from 1960 to 2007 are shown in Fig. S3. The emission centers have shifted from Europe and North America to Asia over the past five decades, in agreement with the trends shown in Fig. 4.

3.4 Mineral sources of Fe

Based on the soil mineralogical data (Journet et al., 2014), the estimated global total emission of Fe from mineral sources ranged from 34.4 to 54.2 Tgyr⁻¹ for 2000–2011, with an average emission of 41.0 Tgyr⁻¹. The modelled average global total emission of dust for 2000–2011 was 1040 Tgyr⁻¹, close to the median of 14 AeroCom Phase I models (1120 Tgyr⁻¹) (Huneus et al., 2011). Our estimated Fe emission from dust is lower than the 55–74 Tgyr⁻¹ reported by Luo et al. (2008) and Ito (2013), mainly because the emission of dust is larger in the models used by these authors. For example, the model used by Luo et al. (2008) simulated a total dust emission of 4313 Tgyr⁻¹ higher than other 13 AeroCom Phase I models (Huneus et al., 2011), including LMDz-INCA. However, the dust emission is very size-dependent, and the emissions should be evaluated by prescribing the size distribution in source regions to the transport models.

Sources, transport and deposition of iron in the global atmosphere

R. Wang et al.

Title Page

Abstract

Introduction

Conclusions

References

Tables

Figures



Back

Close

Full Screen / Esc

Printer-friendly Version

Interactive Discussion



Sources, transport and deposition of iron in the global atmosphere

R. Wang et al.

Title Page

Abstract

Introduction

Conclusions

References

Tables

Figures



Back

Close

Full Screen / Esc

Printer-friendly Version

Interactive Discussion



The average Fe emission density from mineral sources for 2000–2011 is mapped in Fig. 5a. The major source regions include the Sahara Desert, southern Africa, Middle East, northwestern China, southwestern North America, southern South America, and western Australia. The estimated Fe emission map based on the new soil mineralogical data set (Journet et al., 2014) is also compared to that derived using a constant Fe content (3.5 %) (Fig. 5b) as measured by Taylor and McLennan (1985) and widely used in other models (Luo et al., 2008; Mahowald et al., 2009; Ito, 2013). The new mineralogical data set led to a larger Fe emission density over the Sahara, Arabian, and Takla-Makan Deserts, and a lower Fe emission density over the Gobi Desert, reflecting the difference of Fe content of dust relative to 3.5 % (Fig. S2).

3.5 Comparison of Fe emissions with previous studies

Table 1 summarizes the comparison of our estimations of Fe emissions with previous studies (Bertine and Goldberg, 1971; Luo et al., 2008; Ito, 2013). Bertine and Goldberg (1971) estimated the emissions of fifty-one trace elements into the atmosphere from fossil fuel combustion based on a mass-balance method similar to ours. However, due to a lack of data at the time, they assumed that 10 % of all trace elements in fuels was transferred to the atmosphere. This rate is lower than the 30–45 % measured for Fe in recent studies (Yi et al., 2008; Font et al., 2012; Tang et al., 2013). Our estimated Fe emission is approximately twice that the amount found by Bertine and Goldberg (1971) for the same year (1967) after accounting for different removal efficiencies by particle size and control device.

Luo et al. (2008) and Ito (2013) have estimated Fe emissions from the combustion of fossil fuels, biofuels and biomass burning in fine (PM_1) and medium particles (PM_{1-10}). Their estimates of the total Fe emissions (1.7 Tgyr^{-1} for 1996 and 2001) are close to our estimations (1.48 Tgyr^{-1} for 1996 and 1.18 Tgyr^{-1} for 2001). For fossil fuels, Luo et al. (2008) and Ito (2013) estimated Fe emissions based on the particle emission factors and the Fe contents of particles. Their estimates of fossil fuel emissions (0.51 Tgyr^{-1} for 1996 to 0.66 Tgyr^{-1} for 2001) are lower than our estimates (1.18 and

Sources, transport and deposition of iron in the global atmosphere

R. Wang et al.

Title Page

Abstract

Introduction

Conclusions

References

Tables

Figures



Back

Close

Full Screen / Esc

Printer-friendly Version

Interactive Discussion



0.86 Tgyr⁻¹ for the two years, respectively) for the same size class (Table 1). In the method used by Luo et al. (2008) and Ito (2013), the Fe contents of particles are measured in very few studies. For example, for coal burnt in power plants and industry, there are only three measurements in the USA which were used by Luo et al. (2008), reporting an Fe content of 4.5–7.6 % in fine particles and 8.1–9.4 % in coarse particles (Olmez et al., 1988; Smith et al., 1979; Mamane et al., 1986). In addition to large uncertainty in sample collection (Hildemann et al., 1989), the variation of Fe content in particles is large. The measured Fe content in coal fly ash generated by the combustion of bituminous coal in Shanxi Province, China is 10.2–11.9 % (Fu et al., 2012), 40 % higher than the values used by Luo et al. (2008) and Ito (2013). A larger Fe content than that used by Luo et al. (2008) and Ito (2013) was also found for oil/biofuel fly ashes in the measurement by Fu et al. (2012). The large variation of Fe content of particles explains part of the underestimation in the estimates by Luo et al. (2008) and Ito (2013). In addition, Luo et al. (2008) and Ito (2013) estimated that the Fe emission ratio between PM₁ and PM_{1–10} is 1 : 6, compared to 1 : 24 in this study. The emission ratios used by Luo et al. (2008) and Ito (2013) were taken from Bond et al. (2004), which pertained to carbonaceous matter in fine particles but was not justified for Fe (mainly in coarse particles). For biomass burning, our estimates of the total Fe emissions are lower than that by Luo et al. (2008) and Ito (2013). Luo et al. (2008) applied a globally constant Fe : BC emission ratio based on the slope of Fe and BC concentrations observed for aerosols in the Amazon Basin. They assumed that Fe was originated from biomass burning. Note that dust and plant material entrained in fires can also contribute to Fe concentrations, causing a likely overestimation in their estimates according to Luo et al. (2008). Our estimation seems to confirm this fact.

In a recent study focused on East Asia (Lin et al., 2015), the emission of Fe from combustion sources in East Asia in 2007 was estimated to be 7.2 Tgyr⁻¹, far higher than all other studies (Luo et al., 2008; Ito, 2013) and our work (1.6 Tgyr⁻¹). The authors used an alternative method to estimate the emission of Fe based upon the sulfur dioxides (SO₂) emission and the ratio of sulfur and Fe content in fuels. As pointed out by the

4.2 Evaluation of Fe concentrations in surface air

The Fe concentrations attached to aerosols in surface air simulated for pixels of 0.94° latitude by 1.28° longitude were evaluated by 529 measurements obtained between 1990 to 2007. These measurements include data compiled by Mahowald et al. (2009) and Sholkovitz et al. (2012) and our collation of data from peer reviewed studies (Table S3). The modelled Fe concentrations attached to aerosols in surface air, averaged for the months in the year of measurements, are plotted against the measured concentrations (Fig. 7a). The simulated Fe concentrations were grouped into same size range as measurements if the size was specified in the measurements and otherwise they were computed as total concentrations. The modelled spatial pattern matched the observations ($r^2 = 0.52$). Mahowald et al. (2009) compared modelled annual mean Fe concentrations to measurements. They pointed out that the daily measurements from cruises are not as representative as the long-term station measurements. Similarly, a better agreement can be achieved if all cruise measurements are excluded in the comparison ($r^2 = 0.68$) in our study (Fig. 7b).

Three statistical metrics were used to evaluate the model performance (Table 2): the fraction of stations with a deviation within a factor of two (F_2) or five (F_5) and the normalized mean bias (NMB). Globally, 57 and 77 % of the stations were associated with deviations within factors of two and five, respectively, with an NMB of -14% . The model and observations agreed well for East Asia and the Atlantic Ocean, with deviations within a factor of two for 84 and 64 % of stations, respectively. The model overestimated Fe concentrations at some stations over the Atlantic Ocean and the Mediterranean Sea. The model used only one major mode for dust (an initial MMD of $2.5\mu\text{m}$, and a fixed geometric $\sigma = 2.0$), which reproduces the long-range transport and dust optical thickness over the ocean (Schulz et al., 1998). Without more detailed size bins, we assumed that the Fe content of dust and the Fe content of soil in the clay fraction is the same. This assumption is a reasonable approximation for dust transported hundreds of kilometers away from the dust source regions (Formenti et al., 2014), because the lifetime

[Title Page](#)[Abstract](#)[Introduction](#)[Conclusions](#)[References](#)[Tables](#)[Figures](#)[Back](#)[Close](#)[Full Screen / Esc](#)[Printer-friendly Version](#)[Interactive Discussion](#)

**Sources, transport
and deposition of
iron in the global
atmosphere**

R. Wang et al.

Title Page

Abstract

Introduction

Conclusions

References

Tables

Figures



Back

Close

Full Screen / Esc

Printer-friendly Version

Interactive Discussion



of dust is much longer for the clay fraction (up to 13 days) than for the silt (4 to 40 h) and sand (approximately 1 h) fraction (Tegen and Fung, 1994). However, the mineralogy and therefore the density of material is not considered in this simplification. This assumption would lead to an overestimation of the Fe content of dust near the source regions due to the ignored contribution of Fe in the silt and sand fractions (which have lower Fe contents than clay) (Formenti et al., 2014). The overestimation occurs only at stations near continents and downwind of deserts in Fig. 6, indicating that the modelled Fe concentrations over the ocean were not excessively influenced. The model also underestimated Fe concentrations over the Pacific and Southern Oceans, likely due to the uncertainty in dust emissions and to the transport errors in the Southern Hemisphere, which was documented previously (Huneeus et al., 2011; Schulz et al., 2012). Dust emissions over regions of the Southern Hemisphere, such as southern South America and southeastern Africa, require additional investigations.

One should note that modelled monthly mean concentrations were compared to daily measurements (e.g. measured by cruises) due to a lack of detailed date information in measurements. It also caused some discrepancies between model and observations. As pointed out by Mahowald et al. (2009), some cruise measurements were sensitive to episodic dust events. Mahowald et al. (2009) compared the modelled annual mean Fe concentrations to daily measurements, leading to a potential deviation by a factor up to 10. We also expected such a bias in this study, even though we were comparing modelled monthly Fe concentrations to all measurements. To address this influence, we compared modelled daily Fe concentrations to those from some cruise measurements with detailed date information available (Baker et al., 2006; Chen and Siefert, 2004). As illustrated in Fig. 8, particularly in Fig. 8a and b, the variation of daily concentrations could be well captured by the model. These variations were attenuated when using modelled monthly mean Fe concentrations. This agreement lends support to the estimation of annual mean Fe concentrations and thus Fe deposition in our study.

4.3 Fe concentrations over the Atlantic Ocean

The modelled Fe concentrations attached to aerosols in air near the Atlantic Ocean were compared against 296 transect cruise measurements for 2003–2008 (Baker et al., 2013) (Fig. 9). The zonal distribution of Fe concentrations was generally captured by the model ($r^2 = 0.50$). However, the model overestimated the Fe concentrations in the band between 10 and 20° N, because Fe content of the clay fraction was extrapolated to all dust types, leading to an overestimation of Fe concentrations at locations near dust source regions (see the discussion above). In addition, the model underestimated Fe concentrations by a factor of two at stations in the band between 40 and 70° S, and this model-data misfit could be reduced when the modelled concentrations were scaled by a higher dust emission in a sensitivity test (Fig. 9), confirming the high degree of uncertainties in dust emissions and transport in the Southern Hemisphere.

The seasonality of modelled Fe concentrations at two long-term monitoring stations on the western margin of the Atlantic Ocean (Bermuda and Barbados) was compared to the observations, collected between 1988 to 1994 during the AEROCE program (Arimoto et al., 1992, 1995, 2003; Huang et al., 1999) and compiled by Sholkovitz et al. (2009). As shown in Fig. 10, the observed seasonal variations of Fe concentrations at these two stations were well represented by the model, with peaks in summer corresponding to dust storms in the Sahara Desert.

4.4 Role of the combustion sources

The estimated total emissions and the spatial distributions of Fe from combustion sources differed from those of previous studies (Table 1 and Fig. 3). The contribution of combustion sources to the Fe concentrations attached to aerosols in surface air is shown in Fig. 11. Large contribution of combustion sources (> 80%) is found in western Europe, southeastern and northeastern China, southern Africa, central South America and eastern and northern North America, in agreement with the spatial distribution of combustion emissions.

limited improvement obtained using the state-of-the-art mineralogical database implied that other factors, such as the dust emission uncertainties and the transport errors, influenced the estimation of Fe from mineral sources. Further studies are needed to constrain the dust emissions in the Southern Hemisphere in the model (Tagliabue et al., 2009; Schulz et al., 2012). The new mineralogical data provided information on the chemical form of the Fe in dust (Journet et al., 2014), which will help the modelling of Fe solubility.

4.6 Size distributions of Fe-containing particles

The particle size of Fe-containing particles is an important factor controlling the lifetime and solubility of Fe (Baker and Jickells, 2006; Mahowald et al., 2009). In LMDZ-INCA, the size distribution of Fe-containing particles was treated as a log-normal distribution with a varied MMD and a fixed geometric σ . Figure 15 shows the spatial distribution of modelled wet MMD of Fe-containing particles in surface air from combustion and mineral sources. The global average wet MMD of Fe-containing particles is 2.60 μm . The figure illustrates that the Fe was mainly attached to coarse particles ($> 5 \mu\text{m}$) in regions dominated by combustion sources, such as in East Asia, South Asia, Europe, eastern and northern North America, South America and southern Africa. By contrast, the wet MMD of Fe-containing particles is 2.2–2.4 μm over the deserts dominated by mineral sources, such as in northern Africa, western Asia and southeastern North America, slightly smaller than the initialized wet MMD for dust.

After particles are emitted into the atmosphere, the size would increase due to uptake of water in hygroscopic growth (Schulz, 2007) and decrease due to preferential sedimentation and wet scavenging of larger particles (Schulz, 2007). For example, the size of Fe in PM_1 emitted from coal combustion increased from 0.3 μm to $> 2 \mu\text{m}$ after being transported away from the source regions. In contrast, the size of Fe in PM_{1-10} emitted from coal combustion in East Asia would increase over the northern Pacific Ocean and decrease over the southern Pacific Ocean, depending on the relative importance of two mechanisms. The size of Fe in $\text{PM}_{>10}$ from coal combustion would

Sources, transport and deposition of iron in the global atmosphere

R. Wang et al.

Title Page

Abstract

Introduction

Conclusions

References

Tables

Figures



Back

Close

Full Screen / Esc

Printer-friendly Version

Interactive Discussion



decrease from 33 μm in the source regions to $< 10 \mu\text{m}$ over the oceans. In general, the size of Fe was larger over the tropical ocean than over the sub-tropical ocean, due to more precipitation over the tropical regions.

There are limited measurements of size distributions of Fe-containing particles. Sun et al. (2004) measured the Fe concentrations in $\text{PM}_{2.5}$ and PM_{10} at three stations in Beijing. The mean $\pm\sigma$ of the $\text{PM}_{2.5}/\text{PM}_{10}$ ratios of Fe was $28.1 \pm 7.8\%$, compared to $33.5 \pm 1.6\%$ in our simulation. Chen and Siefert (2004) measured the Fe concentrations in $\text{PM}_{2.5}$ and total suspended particles (TSP) over the North Atlantic Ocean. The mean $\pm\sigma$ of the $\text{PM}_{2.5}/\text{TSP}$ ratios of Fe was $55.2 \pm 16.8\%$, compared to the $49.9 \pm 0.5\%$ in our simulation.

5 Global Fe deposition

The distribution of annual mean Fe deposition is shown in Fig. 16. Similar to the distribution of annual mean Fe concentrations attached to aerosols in surface air (Fig. 6), the spatial distribution of Fe deposition was dominated by mineral sources. High Fe deposition rates over the ocean were found over the Arabian Sea and the Indian Ocean ($> 100 \text{mgm}^{-2} \text{yr}^{-1}$), followed by the Atlantic Ocean ($10\text{--}100 \text{mgm}^{-2} \text{yr}^{-1}$) and the northern Pacific Ocean ($5\text{--}30 \text{mgm}^{-2} \text{yr}^{-1}$). Mahowald et al. (2009) pointed out that directly measured Fe deposition rates are very limited. We compared the modelled Fe deposition with in situ measurements compiled by Mahowald et al. (2009). The spatial pattern of measured Fe deposition can be generally represented by the model ($r^2 = 0.88$) (Fig. S5). The limited data, however, prevented us from evaluating the modelled deposition rates globally.

6 Global atmospheric Fe budget

The atmospheric Fe budgets from different emission sources are summarized in Table 3. The atmospheric lifetime of Fe is highly dependent on the particle size, emission

Title Page

Abstract

Introduction

Conclusions

References

Tables

Figures



Back

Close

Full Screen / Esc

Printer-friendly Version

Interactive Discussion



is dependent on the condition of combustion sources (Ito, 2015). More measurements of Fe solubility at various sources and open oceans should be conducted to simulate and constrain the Fe solubility in the future work.

In addition, the study by Lin et al. (2015) predicted that 87 and 41 % of the deposition of soluble Fe over the Northwestern Pacific Ocean could be attributed to combustion-related sources when prescribing a solubility of 40 and 4 % for Fe in fly ash, respectively. Their upper estimate agrees well with our prediction that combustion-related sources would contribute 80–95 % to soluble Fe deposition in this region (Fig. 18).

8 Summary and conclusion

We developed a new emission inventory of Fe from combustion sources using Fe contents of fuel and Fe partitioning during combustion, and estimated the emissions of Fe from mineral sources based on a new soil mineralogical database. We calculated the global total Fe emissions of 0.04, 1.32, and 3.72 Tgyr⁻¹ in PM₁, PM_{1–10} and PM_{>10} from combustion sources, respectively. Although the total Fe emissions are similar, the size distributions and the source profiles differ from those in previous studies, which substantially influenced the Fe solubility in aerosols.

We evaluated the estimated new emissions of Fe from combustion and mineral sources. We introduced the estimated Fe emissions in a global transport model running at a resolution of 0.94° latitude by 1.28° longitude. The modelled Fe concentrations attached to aerosols in surface air were compared with 825 measurements worldwide. The measured Fe concentrations were generally predicted by the model, including the spatial distributions of Fe concentrations in each region, the zonal distributions of Fe concentrations over the Atlantic Ocean, and the seasonality of Fe concentrations on the western margin of the Atlantic Ocean. Importantly, agreement was good at stations where the Fe concentrations were dominated by combustion sources, supporting our new estimations of Fe emissions from combustion sources. The new mineralogical data produced modest improvements but provided useful information on the chemical form

Sources, transport and deposition of iron in the global atmosphere

R. Wang et al.

Title Page

Abstract

Introduction

Conclusions

References

Tables

Figures



Back

Close

Full Screen / Esc

Printer-friendly Version

Interactive Discussion



of Fe. An underestimation of Fe concentrations over the oceans in the Southern Hemisphere, however, may confirm the high uncertainty in dust emissions, which deserves further study.

We estimated a total Fe deposition sink of 7.7 Tgyr^{-1} over global oceans, 7.1 % of which originated from combustion sources. The modelled Fe deposition rates were confirmed by a limited number of in situ measurements. Fe deposition rates over most oceanic regions, however, have not been widely measured. The combustion of coal, petroleum and biomass, all with a much higher Fe solubility than dust, contributed considerably to the deposition of Fe over the northern Atlantic and northern Pacific Oceans. We speculate that this large amount of additional input of soluble Fe may have had an impact on the oceanic carbon cycle and the global climate.

**The Supplement related to this article is available online at
doi:10.5194/acpd-15-7645-2015-supplement.**

Acknowledgements. The authors thank Ether/ECCAD for distribution of emission data used in this study. R. Wang was supported by the “FABIO” project, a Marie Curie International Incoming Fellowship from the European Commission. This work was also supported by the European Research Council Synergy Grant IMBALANCE-P (ERC-SyG-2013-610028). The simulations in this work were performed using DSM-CCRT resources under the GENCI (Grand Equipement National de Calcul Intensif) computer time allocation (grant 2014-t2014012201).

References

- Arimoto, R., Duce, R. A., Savoie, D. L., and Prospero, J. M.: Trace-elements in aerosol-particles from Bermuda and Barbados – concentrations, sources and relationships to aerosol sulfate, *J. Atmos. Chem.*, 14, 439–457, doi:10.1007/Bf00115250, 1992.
- Arimoto, R., Duce, R. A., Ray, B. J., Ellis, W. G., Cullen, J. D., and Merrill, J. T.: Trace-elements in the atmosphere over the North-Atlantic, *J. Geophys. Res.-Atmos.*, 100, 1199–1213, doi:10.1029/94jd02618, 1995.

ACPD

15, 7645–7705, 2015

Sources, transport and deposition of iron in the global atmosphere

R. Wang et al.

Title Page

Abstract

Introduction

Conclusions

References

Tables

Figures



Back

Close

Full Screen / Esc

Printer-friendly Version

Interactive Discussion



**Sources, transport
and deposition of
iron in the global
atmosphere**

R. Wang et al.

Title Page

Abstract

Introduction

Conclusions

References

Tables

Figures



Back

Close

Full Screen / Esc

Printer-friendly Version

Interactive Discussion



- Arimoto, R., Duce, R. A., Ray, B. J., and Tomza, U.: Dry deposition of trace elements to the western North Atlantic, *Global Biogeochem. Cy.*, 17, 1010, doi:10.1029/2001gb001406, 2003.
- Baker, A. R. and Jickells, T. D.: Mineral particle size as a control on aerosol iron solubility, *Geophys. Res. Lett.*, 33, L17608, doi:10.1029/2006gl026557, 2006.
- 5 Baker, A. R., Jickells, T. D., Witt, M., and Linge, K. L.: Trends in the solubility of iron, aluminium, manganese and phosphorus in aerosol collected over the Atlantic Ocean, *Mar. Chem.*, 98, 43–58, doi:10.1016/j.marchem.2005.06.004, 2006.
- Baker, A. R., Adams, C., Bell, T. G., Jickells, T. D., and Ganzeveld, L.: Estimation of atmospheric nutrient inputs to the Atlantic Ocean from 50° N to 50° S based on large-scale field sampling: iron and other dust-associated elements, *Global Biogeochem. Cy.*, 27, 755–767, doi:10.1002/Gbc.20062, 2013.
- 10 Balkanski, Y.: L'Influence des Aérosols sur le Climat, Thèse d'Habilitation à Diriger des Recherches, Université de Versailles Saint-Quentin, Saint-Quentin-en-Yvelines, 2011.
- Balkanski, Y., Schulz, M., Claquin, T., Moulin, C., and Ginoux, P.: Global emissions of mineral aerosol: formulation and validation using satellite imagery, in: *Emissions of Atmospheric Trace Compounds*, edited by: Granier, C., Artaxo, P., and Reeves, C., *Advances in Global Change Research*, Springer Netherlands, Dordrecht, the Netherlands, 239–267, 2004.
- 15 Balkanski, Y., Schulz, M., Claquin, T., and Guibert, S.: Reevaluation of Mineral aerosol radiative forcings suggests a better agreement with satellite and AERONET data, *Atmos. Chem. Phys.*, 7, 81–95, doi:10.5194/acp-7-81-2007, 2007.
- Balkanski, Y., Myhre, G., Gauss, M., Rädel, G., Highwood, E. J., and Shine, K. P.: Direct radiative effect of aerosols emitted by transport: from road, shipping and aviation, *Atmos. Chem. Phys.*, 10, 4477–4489, doi:10.5194/acp-10-4477-2010, 2010.
- Bertine, K. K. and Goldberg, E. D.: Fossil fuel combustion and the major sedimentary cycle, *Science*, 173, 233–235, doi:10.1126/science.173.3993.233, 1971.
- 25 Bettinelli, M., Spezia, S., Baroni, U., and Bizzarri, G.: Determination of trace-elements in fuel oils by inductively-coupled plasma-mass spectrometry after acid mineralization of the sample in a microwave-oven, *J. Anal. Atom. Spectrom.*, 10, 555–560, doi:10.1039/Ja9951000555, 1995.
- 30 Bond, T. C., Streets, D. G., Yarber, K. F., Nelson, S. M., Woo, J. H., and Klimont, Z.: A technology-based global inventory of black and organic carbon emissions from combustion, *J. Geophys. Res.-Atmos.*, 109, D14203, doi:10.1029/2003jd003697, 2004.

**Sources, transport
and deposition of
iron in the global
atmosphere**

R. Wang et al.

Title Page

Abstract

Introduction

Conclusions

References

Tables

Figures



Back

Close

Full Screen / Esc

Printer-friendly Version

Interactive Discussion



- Bond, T. C., Bhardwaj, E., Dong, R., Jogani, R., Jung, S. K., Roden, C., Streets, D. G., and Trautmann, N. M.: Historical emissions of black and organic carbon aerosol from energy-related combustion, 1850–2000, *Global Biogeochem. Cy.*, 21, GB2018, doi:10.1029/2006gb002840, 2007.
- 5 Bowie, A. R., Lannuzel, D., Remenyi, T. A., Wagener, T., Lam, P. J., Boyd, P. W., Guieu, C., Townsend, A. T., and Trull, T. W.: Biogeochemical iron budgets of the Southern Ocean south of Australia: decoupling of iron and nutrient cycles in the subantarctic zone by the summer-time supply, *Global Biogeochem. Cy.*, 23, GB4034, doi:10.1029/2009gb003500, 2009.
- 10 Boyd, P. W., Watson, A. J., Law, C. S., Abraham, E. R., Trull, T., Murdoch, R., Bakker, D. C. E., Bowie, A. R., Buesseler, K. O., Chang, H., Charette, M., Croot, P., Downing, K., Frew, R., Gall, M., Hadfield, M., Hall, J., Harvey, M., Jameson, G., LaRoche, J., Liddicoat, M., Ling, R., Maldonado, M. T., McKay, R. M., Nodder, S., Pickmere, S., Pridmore, R., Rintoul, S., Safi, K., Sutton, P., Strzepek, R., Tanneberger, K., Turner, S., Waite, A., and Zeldis, J.: A mesoscale phytoplankton bloom in the polar Southern Ocean stimulated by iron fertilization, *Nature*, 407, 695–702, doi:10.1038/35037500, 2000.
- 15 Chalot, M., Blaudez, D., Rogaume, Y., Provent, A. S., and Pascual, C.: Fate of trace elements during the combustion of phytoremediation wood, *Environ. Sci. Technol.*, 46, 13361–13369, doi:10.1021/Es3017478, 2012.
- Chaves, E. S., de Loos-Vollebregt, M. T. C., Curtius, A. J., and Vanhaecke, F.: Determination of trace elements in biodiesel and vegetable oil by inductively coupled plasma optical emission spectrometry following alcohol dilution, *Spectrochim. Acta B*, 66, 733–739, doi:10.1016/j.sab.2011.09.006, 2011.
- 20 Chen, H., Laskin, A., Baltusaitis, J., Gorski, C. A., Scherer, M. M., and Grassian, V. H.: Coal fly ash as a source of iron in atmospheric dust, *Environ. Sci. Technol.*, 46, 2112–2120, doi:10.1021/Es204102f, 2012.
- 25 Chen, Y. and Siefert, R. L.: Seasonal and spatial distributions and dry deposition fluxes of atmospheric total and labile iron over the tropical and subtropical North Atlantic Ocean, *J. Geophys. Res.-Atmos.*, 109, D09305, doi:10.1029/2003jd003958, 2004.
- Chen, Y. J., Zhi, G. R., Feng, Y. L., Fu, J. M., Feng, J. L., Sheng, G. Y., and Simoneit, B. R. T.: Measurements of emission factors for primary carbonaceous particles from residential raw-coal combustion in China, *Geophys. Res. Lett.*, 33, L20815, doi:10.1029/2006gl026966, 2006.
- 30

**Sources, transport
and deposition of
iron in the global
atmosphere**

R. Wang et al.

Title Page

Abstract

Introduction

Conclusions

References

Tables

Figures

◀

▶

◀

▶

Back

Close

Full Screen / Esc

Printer-friendly Version

Interactive Discussion



Chen, Y. L., Wang, R., Shen, H. Z., Li, W., Chen, H., Huang, Y., Zhang, Y. Y., Chen, Y. C., Su, S., Lin, N., Liu, J., Li, B. G., Wang, X. L., Liu, W. X., Coveney, R. M., and Tao, S.: Global mercury emissions from combustion in light of international fuel trading, *Environ. Sci. Technol.*, 48, 1727–1735, doi:10.1021/Es404110f, 2014.

5 Chuang, P. Y., Duvall, R. M., Shafer, M. M., and Schauer, J. J.: The origin of water soluble particulate iron in the Asian atmospheric outflow, *Geophys. Res. Lett.*, 32, L07813, doi:10.1029/2004gl021946, 2005.

Conway, T. M. and John, S. G.: Quantification of dissolved iron sources to the North Atlantic Ocean, *Nature*, 511, 212–215, doi:10.1038/Nature13482, 2014.

10 Duce, R. A. and Tindale, N. W.: Atmospheric transport of iron and its deposition in the ocean, *Limnol. Oceanogr.*, 36, 1715–1726, 1991.

Espinosa, A. J. F., Rodriguez, M. T., de la Rosa, F. J. B., and Sanchez, J. C. J.: A chemical speciation of trace metals for fine urban particles, *Atmos. Environ.*, 36, 773–780, 2002.

Fan, S. M., Moxim, W. J., and Levy, H.: Aeolian input of bioavailable iron to the ocean, *Geophys. Res. Lett.*, 33, L07602, doi:10.1029/2005gl024852, 2006.

Font, O., Cordoba, P., Leiva, C., Romeo, L. M., Bolea, I., Guedea, I., Moreno, N., Querol, X., Fernandez, C., and Diez, L. I.: Fate and abatement of mercury and other trace elements in a coal fluidised bed oxy combustion pilot plant, *Fuel*, 95, 272–281, doi:10.1016/j.fuel.2011.12.017, 2012.

20 Formenti, P., Caquineau, S., Desboeufs, K., Klaver, A., Chevaillier, S., Journet, E., and Rajot, J. L.: Mapping the physico-chemical properties of mineral dust in western Africa: mineralogical composition, *Atmos. Chem. Phys.*, 14, 10663–10686, doi:10.5194/acp-14-10663-2014, 2014.

Fu, H. B., Lin, J., Shang, G. F., Dong, W. B., Grassian, V. H., Carmichael, G. R., Li, Y., and Chen, J. M.: Solubility of iron from combustion source particles in acidic media linked to iron speciation, *Environ. Sci. Technol.*, 46, 11119–11127, doi:10.1021/Es302558m, 2012.

25 Fung, I. Y., Meyn, S. K., Tegen, I., Doney, S. C., John, J. G., and Bishop, J. K. B.: Iron supply and demand in the upper ocean, *Global Biogeochem. Cy.*, 14, 281–295, doi:10.1029/1999gb900059, 2000.

30 Gao, Y., Kaufman, Y. J., Tanre, D., Kolber, D., and Falkowski, P. G.: Seasonal distributions of aeolian iron fluxes to the global ocean, *Geophys. Res. Lett.*, 28, 29–32, doi:10.1029/2000gl011926, 2001.

Sources, transport and deposition of iron in the global atmosphere

R. Wang et al.

Title Page

Abstract

Introduction

Conclusions

References

Tables

Figures



Back

Close

Full Screen / Esc

Printer-friendly Version

Interactive Discussion



- Granier, C., Bessagnet, B., Bond, T., D'Angiola, A., van der Gon, H. D., Frost, G. J., Heil, A., Kaiser, J. W., Kinne, S., Klimont, Z., Kloster, S., Lamarque, J. F., Liousse, C., Masui, T., Meleux, F., Mieville, A., Ohara, T., Raut, J. C., Riahi, K., Schultz, M. G., Smith, S. J., Thompson, A., van Aardenne, J., van der Werf, G. R., and van Vuuren, D. P.: Evolution of anthropogenic and biomass burning emissions of air pollutants at global and regional scales during the 1980–2010 period, *Climatic Change*, 109, 163–190, doi:10.1007/s10584-011-0154-1, 2011.
- Gregg, W. W., Ginoux, P., Schopf, P. S., and Casey, N. W.: Phytoplankton and iron: validation of a global three-dimensional ocean biogeochemical model, *Deep-Sea Res. Pt. II*, 50, 3143–3169, doi:10.1016/j.dsr2.2003.07.013, 2003.
- Grubler, A., Nakicenovic, N., and Victor, D. G.: Dynamics of energy technologies and global change, *Energ. Policy*, 27, 247–280, doi:10.1016/S0301-4215(98)00067-6, 1999.
- Guelle, W., Balkanski, Y. J., Schulz, M., Marticorena, B., Bergametti, G., Moulin, C., Arimoto, R., and Perry, K. D.: Modeling the atmospheric distribution of mineral aerosol: comparison with ground measurements and satellite observations for yearly and synoptic timescales over the North Atlantic, *J. Geophys. Res.-Atmos.*, 105, 1997–2012, doi:10.1029/1999jd901084, 2000.
- Guieu, C., Bonnet, S., Wagener, T., and Loye-Pilot, M. D.: Biomass burning as a source of dissolved iron to the open ocean?, *Geophys. Res. Lett.*, 32, L19608, doi:10.1029/2005gl022962, 2005.
- Hand, J. L., Mahowald, N. M., Chen, Y., Siefert, R. L., Luo, C., Subramaniam, A., and Fung, I.: Estimates of atmospheric-processed soluble iron from observations and a global mineral aerosol model: biogeochemical implications, *J. Geophys. Res.-Atmos.*, 109, D17205, doi:10.1029/2004jd004574, 2004.
- Hauglustaine, D. A., Hourdin, F., Jourdain, L., Filiberti, M. A., Walters, S., Lamarque, J. F., and Holland, E. A.: Interactive chemistry in the Laboratoire de Meteorologie Dynamique general circulation model: description and background tropospheric chemistry evaluation, *J. Geophys. Res.-Atmos.*, 109, D04314, doi:10.1029/2003jd003957, 2004.
- Hildemann, L. M., Cass, G. R., and Markowski, G. R.: A dilution stack sampler for collection of organic aerosol emissions – design, characterization and field-tests, *Aerosol Sci. Tech.*, 10, 193–204, doi:10.1080/02786828908959234, 1989.
- Holscher, D., Moller, R. F., Denich, M., and Folster, H.: Nutrient input-output budget of shifting agriculture in Eastern Amazonia, *Nutr. Cycl. Agroecosys.*, 47, 49–57, 1997.

**Sources, transport
and deposition of
iron in the global
atmosphere**

R. Wang et al.

Title Page

Abstract

Introduction

Conclusions

References

Tables

Figures



Back

Close

Full Screen / Esc

Printer-friendly Version

Interactive Discussion



- Hourdin, F. and Issartel, J. P.: Sub-surface nuclear tests monitoring through the CTBT xenon network, *Geophys. Res. Lett.*, 27, 2245–2248, doi:10.1029/1999gl010909, 2000.
- Hourdin, F., Musat, I., Bony, S., Braconnot, P., Codron, F., Dufresne, J. L., Fairhead, L., Filiberti, M. A., Friedlingstein, P., Grandpeix, J. Y., Krinner, G., Levan, P., Li, Z. X., and Lott, F.: The LMDZ4 general circulation model: climate performance and sensitivity to parametrized physics with emphasis on tropical convection, *Clim. Dynam.*, 27, 787–813, doi:10.1007/s00382-006-0158-0, 2006.
- Huang, S. L., Rahn, K. A., Arimoto, R., Graustein, W. C., and Turekian, K. K.: Semi-annual cycles of pollution at Bermuda, *J. Geophys. Res.-Atmos.*, 104, 30309–30317, doi:10.1029/1999jd900801, 1999.
- Huneus, N., Schulz, M., Balkanski, Y., Griesfeller, J., Prospero, J., Kinne, S., Bauer, S., Boucher, O., Chin, M., Dentener, F., Diehl, T., Easter, R., Fillmore, D., Ghan, S., Ginoux, P., Grini, A., Horowitz, L., Koch, D., Krol, M. C., Landing, W., Liu, X., Mahowald, N., Miller, R., Morcrette, J.-J., Myhre, G., Penner, J., Perlwitz, J., Stier, P., Takemura, T., and Zender, C. S.: Global dust model intercomparison in AeroCom phase I, *Atmos. Chem. Phys.*, 11, 7781–7816, doi:10.5194/acp-11-7781-2011, 2011.
- Ingerslev, M., Skov, S., Sevel, L., and Pedersen, L. B.: Element budgets of forest biomass combustion and ash fertilisation – a Danish case-study, *Biomass Bioenerg.*, 35, 2697–2704, doi:10.1016/j.biombioe.2011.03.018, 2011.
- International Energy Agency: *Energy Statistics of Non-OECD Countries 1970–2006*, Paris, 2008.
- Ito, A.: Global modeling study of potentially bioavailable iron input from shipboard aerosol sources to the ocean, *Global Biogeochem. Cy.*, 27, 1–10, doi:10.1029/2012gb004378, 2013.
- Ito, A.: Atmospheric processing of combustion aerosols as a source of bioavailable iron, *Environ. Sci. Technol. Lett.*, 2, 70–75, doi:10.1021/acs.estlett.5b00007, 2015.
- Ito, A. and Feng, Y.: Role of dust alkalinity in acid mobilization of iron, *Atmos. Chem. Phys.*, 10, 9237–9250, doi:10.5194/acp-10-9237-2010, 2010.
- Ito, A. and Xu, L.: Response of acid mobilization of iron-containing mineral dust to improvement of air quality projected in the future, *Atmos. Chem. Phys.*, 14, 3441–3459, doi:10.5194/acp-14-3441-2014, 2014.
- Johnson, K. S., Gordon, R. M., and Coale, K. H.: What controls dissolved iron concentrations in the world ocean?, *Mar. Chem.*, 57, 137–161, doi:10.1016/S0304-4203(97)00043-1, 1997.

Sources, transport and deposition of iron in the global atmosphere

R. Wang et al.

Title Page

Abstract

Introduction

Conclusions

References

Tables

Figures



Back

Close

Full Screen / Esc

Printer-friendly Version

Interactive Discussion



Johnson, M., Edwards, R., Frenk, C. A., and Masera, O.: In-field greenhouse gas emissions from cookstoves in rural Mexican households, *Atmos. Environ.*, 42, 1206–1222, doi:10.1016/j.atmosenv.2007.10.034, 2008.

Journet, E., Desboeufs, K. V., Caquineau, S., and Colin, J. L.: Mineralogy as a critical factor of dust iron solubility, *Geophys. Res. Lett.*, 35, L07805, doi:10.1029/2007gl031589, 2008.

Journet, E., Balkanski, Y., and Harrison, S. P.: A new data set of soil mineralogy for dust-cycle modeling, *Atmos. Chem. Phys.*, 14, 3801–3816, doi:10.5194/acp-14-3801-2014, 2014.

Kim, Y., Kim, N. Y., Park, S. Y., Lee, D. K., and Lee, J. H.: Classification and individualization of used engine oils using elemental composition and discriminant analysis, *Forensic Sci. Int.*, 230, 58–67, doi:10.1016/j.forsciint.2013.01.013, 2013.

Kittelson, D. B.: Engines and nanoparticles: a review, *J. Aerosol Sci.*, 29, 575–588, doi:10.1016/S0021-8502(97)10037-4, 1998.

Krinner, G., Viovy, N., de Noblet-Ducoudre, N., Ogee, J., Polcher, J., Friedlingstein, P., Ciais, P., Sitch, S., and Prentice, I. C.: A dynamic global vegetation model for studies of the coupled atmosphere-biosphere system, *Global Biogeochem. Cy.*, 19, GB1015, doi:10.1029/2003gb002199, 2005.

Laclau, J. P., Sama-Poumba, W., Nzila, J. D., Bouillet, J. P., and Ranger, J.: Biomass and nutrient dynamics in a littoral savanna subjected to annual fires in Congo, *Acta Oecol.*, 23, 41–50, doi:10.1016/S1146-609x(02)01132-3, 2002.

Lamarque, J.-F., Bond, T. C., Eyring, V., Granier, C., Heil, A., Klimont, Z., Lee, D., Liousse, C., Mieville, A., Owen, B., Schultz, M. G., Shindell, D., Smith, S. J., Stehfest, E., Van Aardenne, J., Cooper, O. R., Kainuma, M., Mahowald, N., McConnell, J. R., Naik, V., Riahi, K., and van Vuuren, D. P.: Historical (1850–2000) gridded anthropogenic and biomass burning emissions of reactive gases and aerosols: methodology and application, *Atmos. Chem. Phys.*, 10, 7017–7039, doi:10.5194/acp-10-7017-2010, 2010.

Latva-Somppi, J., Kauppinen, E. I., Valmari, T., Ahonen, P., Gurav, A. S., Kodas, T. T., and Johanson, B.: The ash formation during co-combustion of wood and sludge in industrial fluidized bed boilers, *Fuel Process. Technol.*, 54, 79–94, doi:10.1016/S0378-3820(97)00061-1, 1998.

Lee, S., Baumann, K., Schauer, J. J., Sheesley, R. J., Naeher, L. P., Meinardi, S., Blake, D. R., Edgerton, E. S., Russell, A. G., and Clements, M.: Gaseous and particulate emissions from prescribed burning in Georgia, *Environ. Sci. Technol.*, 39, 9049–9056, doi:10.1021/Es051583I, 2005.

Sources, transport and deposition of iron in the global atmosphere

R. Wang et al.

Title Page

Abstract

Introduction

Conclusions

References

Tables

Figures



Back

Close

Full Screen / Esc

Printer-friendly Version

Interactive Discussion



- Li, X. G., Wang, S. X., Duan, L., Hao, J., Li, C., Chen, Y. S., and Yang, L.: Particulate and trace gas emissions from open burning of wheat straw and corn stover in China, *Environ. Sci. Technol.*, 41, 6052–6058, doi:10.1021/Es0705137, 2007.
- Lin, Y. C., Chen, J. P., Ho, T. Y., and Tsai, I. C.: Atmospheric iron deposition in the northwestern Pacific Ocean and its adjacent marginal seas: the importance of coal burning, *Global Biogeochem. Cy.*, 29, 1–22, doi:10.1002/2013GB004795, 2015.
- Linak, W. P. and Miller, C. A.: Comparison of particle size distributions and elemental partitioning from the combustion of pulverized coal and residual fuel oil, *J. Air Waste Manage.*, 50, 1532–1544, 2000.
- Luo, C., Mahowald, N. M., and del Corral, J.: Sensitivity study of meteorological parameters on mineral aerosol mobilization, transport, and distribution, *J. Geophys. Res.-Atmos.*, 108, 4447, doi:10.1029/2003jd003483, 2003.
- Luo, C., Mahowald, N. M., Meskhidze, N., Chen, Y., Siefert, R. L., Baker, A. R., and Johansen, A. M.: Estimation of iron solubility from observations and a global aerosol model, *J. Geophys. Res.-Atmos.*, 110, 4447, doi:10.1029/2005jd006059, 2005.
- Luo, C., Mahowald, N., Bond, T., Chuang, P. Y., Artaxo, P., Siefert, R., Chen, Y., and Schauer, J.: Combustion iron distribution and deposition, *Global Biogeochem. Cy.*, 22, D23307, doi:10.1029/2007gb002964, 2008.
- Mackensen, J., Holscher, D., Klinge, R., and Folster, H.: Nutrient transfer to the atmosphere by burning of debris in eastern Amazonia, *Forest Ecol. Manag.*, 86, 121–128, doi:10.1016/S0378-1127(96)03790-5, 1996.
- Mahowald, N. M., Baker, A. R., Bergametti, G., Brooks, N., Duce, R. A., Jickells, T. D., Kubilay, N., Prospero, J. M., and Tegen, I.: Atmospheric global dust cycle and iron inputs to the ocean, *Global Biogeochem. Cy.*, 19, GB1012, doi:10.1029/2004gb002402, 2005.
- Mahowald, N. M., Engelstaedter, S., Luo, C., Sealy, A., Artaxo, P., Benitez-Nelson, C., Bonnet, S., Chen, Y., Chuang, P. Y., Cohen, D. D., Dulac, F., Herut, B., Johansen, A. M., Kubilay, N., Losno, R., Maenhaut, W., Paytan, A., Prospero, J. A., Shank, L. M., and Siefert, R. L.: Atmospheric iron deposition: global distribution, variability, and human perturbations, *Annu. Rev. Mar. Sci.*, 1, 245–278, doi:10.1146/annurev.marine.010908.163727, 2009.
- Mahowald, N., Lindsay, K., Rothenberg, D., Doney, S. C., Moore, J. K., Thornton, P., Rander-son, J. T., and Jones, C. D.: Desert dust and anthropogenic aerosol interactions in the Community Climate System Model coupled-carbon-climate model, *Biogeosciences*, 8, 387–414, doi:10.5194/bg-8-387-2011, 2011.

**Sources, transport
and deposition of
iron in the global
atmosphere**

R. Wang et al.

Title Page

Abstract

Introduction

Conclusions

References

Tables

Figures



Back

Close

Full Screen / Esc

Printer-friendly Version

Interactive Discussion

- Mamane, Y., Miller, J. L., and Dzubay, T. G.: Characterization of individual fly-ash particles emitted from coal-fired and oil-fired power-plants, *Atmos. Environ.*, 20, 2125–2135, doi:10.1016/0004-6981(86)90306-9, 1986.
- Martin, J. H.: Glacial-interglacial CO₂ change: the iron hypothesis, *Paleoceanography*, 5, 1–13, doi:10.1029/Pa005i001p00001, 1990.
- Martin, J. H., Gordon, R. M., and Fitzwater, S. E.: The case for iron, *Limnol. Oceanogr.*, 36, 1793–1802, 1991.
- Meij, R.: Trace-element behavior in coal-fired power-plants, *Fuel Process. Technol.*, 39, 199–217, doi:10.1016/0378-3820(94)90180-5, 1994.
- Ministry of Environmental Protection of the People's Republic of China: China Environment Yearbook 2008, China Environment Yearbook Inc., Beijing, 2008.
- Moore, C. M., Mills, M. M., Arrigo, K. R., Berman-Frank, I., Bopp, L., Boyd, P. W., Galbraith, E. D., Geider, R. J., Guieu, C., Jaccard, S. L., Jickells, T. D., La Roche, J., Lenton, T. M., Mahowald, N. M., Maranon, E., Marinov, I., Moore, J. K., Nakatsuka, T., Oschlies, A., Saito, M. A., Thingstad, T. F., Tsuda, A., and Ulloa, O.: Processes and patterns of oceanic nutrient limitation, *Nat. Geosci.*, 6, 701–710, doi:10.1038/Ngeo1765, 2013.
- Moore, J. K., Doney, S. C., and Lindsay, K.: Upper ocean ecosystem dynamics and iron cycling in a global three-dimensional model, *Global Biogeochem. Cy.*, 18, GB4025, doi:10.1029/2004gb002220, 2004.
- Nardoslawsky, M. and Obernberger, I.: From waste to raw material – the route from biomass to wood ash for cadmium and other heavy metals, *J. Hazard. Mater.*, 50, 157–168, doi:10.1016/0304-3894(96)01785-2, 1996.
- Nickovic, S., Vukovic, A., Vujadinovic, M., Djurdjevic, V., and Pejanovic, G.: Technical Note: High-resolution mineralogical database of dust-productive soils for atmospheric dust modeling, *Atmos. Chem. Phys.*, 12, 845–855, doi:10.5194/acp-12-845-2012, 2012.
- Nickovic, S., Vukovic, A., and Vujadinovic, M.: Atmospheric processing of iron carried by mineral dust, *Atmos. Chem. Phys.*, 13, 9169–9181, doi:10.5194/acp-13-9169-2013, 2013.
- Obernberger, I., Biedermann, F., Widmann, W., and Riedl, R.: Concentrations of inorganic elements in biomass fuels and recovery in the different ash fractions, *Biomass Bioenerg.*, 12, 211–224, doi:10.1016/S0961-9534(96)00051-7, 1997.
- Olmez, I., Sheffield, A. E., Gordon, G. E., Houck, J. E., Pritchett, L. C., Cooper, J. A., Dzubay, T. G., and Bennett, R. L.: Compositions of particles from selected sources in

Sources, transport and deposition of iron in the global atmosphere

R. Wang et al.

Title Page

Abstract

Introduction

Conclusions

References

Tables

Figures



Back

Close

Full Screen / Esc

Printer-friendly Version

Interactive Discussion



Philadelphia for receptor modeling applications, JAPCA J. Air Waste Ma., 38, 1392–1402, 1988.

Pivello, V. R. and Coutinho, L. M.: Transfer of macro-nutrients to the atmosphere during experimental burnings in an open cerrado (Brazilian Savanna), J. Trop. Ecol., 8, 487–497, doi:10.1017/S0266467400006829, 1992.

Querol, X., Fernandez-Turiel, J. L., and Lopez Soler, A.: Trace-elements in coal and their behavior during combustion in a large power-station, Fuel, 74, 331–343, doi:10.1016/0016-2361(95)93464-O, 1995.

Raison, R. J., Khanna, P. K., and Woods, P. V.: Mechanisms of element transfer to the atmosphere during vegetation fires, Can. J. Forest Res., 15, 132–140, doi:10.1139/X85-022, 1985.

Reddy, M. S., Basha, S. B., Joshi, H. V., and Jha, B.: Evaluation of the emission characteristics of trace metals from coal and fuel oil fired power plants and their fate during combustion, J. Hazard. Mater., 123, 242–249, doi:10.1016/j.jhazmat.2005.04.008, 2005.

Ridgwell, A. J. and Watson, A. J.: Feedback between aeolian dust, climate, and atmospheric CO₂ in glacial time, Paleoclimatology, 17, GB4028, doi:10.1029/2001pa000729, 2002.

Sager, M.: Trace and nutrient elements in manure, dung and compost samples in Austria, Soil Biol. Biochem., 39, 1383–1390, doi:10.1016/j.soilbio.2006.12.015, 2007.

Schroth, A. W., Crusius, J., Sholkovitz, E. R., and Bostick, B. C.: Iron solubility driven by speciation in dust sources to the ocean, Nat. Geosci., 2, 337–340, doi:10.1038/Ngeo501, 2009.

Schulz, M.: Constraining Model Estimates of the Aerosol Radiative Forcing, Thèse d'Habilitation à Diriger des Recherches, Université Pierre et Marie Curie, Paris VI, 2007.

Schulz, M., Balkanski, Y. J., Guelle, W., and Dulac, F.: Role of aerosol size distribution and source location in a three-dimensional simulation of a Saharan dust episode tested against satellite-derived optical thickness, J. Geophys. Res.-Atmos., 103, 10579–10592, doi:10.1029/97jd02779, 1998.

Schultz, M. G., Heil, A., Hoelzemann, J. J., Spessa, A., Thonicke, K., Goldammer, J. G., Held, A. C., Pereira, J. M. C., and van het Bolscher, M.: Global wildland fire emissions from 1960 to 2000, Global Biogeochem. Cy., 22, 1059, doi:10.1029/2007gb003031, 2008.

Schulz, M., Prospero, J. M., Baker, A. R., Dentener, F., Ickes, L., Liss, P. S., Mahowald, N. M., Nickovic, S., Garcia-Pando, C. P., Rodriguez, S., Sarin, M., Tegen, I., and Duce, R. A.: Atmospheric transport and deposition of mineral dust to the ocean: implications for research needs, Environ. Sci. Technol., 46, 10390–10404, doi:10.1021/Es300073u, 2012.

Sources, transport
and deposition of
iron in the global
atmosphere

R. Wang et al.

Title Page

Abstract

Introduction

Conclusions

References

Tables

Figures

◀

▶

◀

▶

Back

Close

Full Screen / Esc

Printer-friendly Version

Interactive Discussion

- Sedwick, P. N., Sholkovitz, E. R., and Church, T. M.: Impact of anthropogenic combustion emissions on the fractional solubility of aerosol iron: evidence from the Sargasso Sea, *Geochim. Geophys. Geos.*, 8, GB2002, doi:10.1029/2007gc001586, 2007.
- Shen, G. F., Yang, Y. F., Wang, W., Tao, S., Zhu, C., Min, Y. J., Xue, M. A., Ding, J. N., Wang, B., Wang, R., Shen, H. Z., Li, W., Wang, X. L., and Russell, A. G.: Emission factors of particulate matter and elemental carbon for crop residues and coals burned in typical household stoves in China, *Environ. Sci. Technol.*, 44, 7157–7162, doi:10.1021/Es101313y, 2010.
- Shen, G. F., Wei, S. Y., Wei, W., Zhang, Y. Y., Min, Y. J., Wang, B., Wang, R., Li, W., Shen, H. Z., Huang, Y., Yang, Y. F., Wang, W., Wang, X. L., Wang, X. J., and Tao, S.: Emission factors, size distributions, and emission inventories of carbonaceous particulate matter from residential wood combustion in rural China, *Environ. Sci. Technol.*, 46, 4207–4214, doi:10.1021/Es203957u, 2012.
- Sholkovitz, E. R., Sedwick, P. N., and Church, T. M.: Influence of anthropogenic combustion emissions on the deposition of soluble aerosol iron to the ocean: empirical estimates for island sites in the North Atlantic, *Geochim. Cosmochim. Ac.*, 73, 3981–4003, doi:10.1016/j.gca.2009.04.029, 2009.
- Sholkovitz, E. R., Sedwick, P. N., Church, T. M., Baker, A. R., and Powell, C. F.: Fractional solubility of aerosol iron: synthesis of a global-scale data set, *Geochim. Cosmochim. Ac.*, 89, 173–189, doi:10.1016/j.gca.2012.04.022, 2012.
- Slinn, S. A. and Slinn, W. G. N.: Predictions for particle deposition on natural waters, *Atmos. Environ.*, 14, 1013–1016, doi:10.1016/0004-6981(80)90032-3, 1980.
- Smith, R. D., Campbell, J. A., and Nielson, K. K.: Characterization and formation of sub-micron particles in coal-fired plants, *Atmos. Environ.*, 13, 607–617, doi:10.1016/0004-6981(79)90189-6, 1979.
- Sun, Y. L., Zhuang, G. S., Ying, W., Han, L. H., Guo, J. H., Mo, D., Zhang, W. J., Wang, Z. F., and Hao, Z. P.: The air-borne particulate pollution in Beijing – concentration, composition, distribution and sources, *Atmos. Environ.*, 38, 5991–6004, doi:10.1016/j.atmosenv.2004.07.009, 2004.
- Tagliabue, A., Bopp, L., and Aumont, O.: Evaluating the importance of atmospheric and sedimentary iron sources to Southern Ocean biogeochemistry, *Geophys. Res. Lett.*, 36, Q10Q06, doi:10.1029/2009gl038914, 2009.

Sources, transport and deposition of iron in the global atmosphere

R. Wang et al.

Title Page

Abstract

Introduction

Conclusions

References

Tables

Figures



Back

Close

Full Screen / Esc

Printer-friendly Version

Interactive Discussion



Tang, Q., Liu, G. J., Zhou, C. C., and Sun, R. Y.: Distribution of trace elements in feed coal and combustion residues from two coal-fired power plants at Huainan, Anhui, China, *Fuel*, 107, 315–322, doi:10.1016/j.fuel.2013.01.009, 2013.

Taylor, S. R. and McLennan, S. M.: *The Continental Crust: Its Composition and Evolution*, Blackwell, Malden, MA, 312 pp., 1985.

Tegen, I. and Fung, I.: Modeling of mineral dust in the atmosphere – sources, transport, and optical-thickness, *J. Geophys. Res.-Atmos.*, 99, 22897–22914, doi:10.1029/94jd01928, 1994.

Tewalt, S. J., Belkin, H. E., SanFilipo, J. R., Merrill, M. D., Palmer, C. A., Warwick, P. D., Karlsen, A. W., Finkelman, R. B., and Park, A. J.: Chemical analyses in the World coal quality inventory, version 1: U. S. Geological Survey Open-File Report 2010-1196, available at: <http://pubs.usgs.gov/of/2010/1196/> (last access: 10 March 2015), 2010.

Valmari, T., Lind, T. M., Kauppinen, E. I., Sfiris, G., Nilsson, K., and Maenhaut, W.: Field study on ash behavior during circulating fluidized-bed combustion of biomass. 1. Ash formation, *Energ. Fuel.*, 13, 379–389, doi:10.1021/Ef980085d, 1999.

van der Werf, G. R., Randerson, J. T., Giglio, L., Collatz, G. J., Mu, M., Kasibhatla, P. S., Morton, D. C., DeFries, R. S., Jin, Y., and van Leeuwen, T. T.: Global fire emissions and the contribution of deforestation, savanna, forest, agricultural, and peat fires (1997–2009), *Atmos. Chem. Phys.*, 10, 11707–11735, doi:10.5194/acp-10-11707-2010, 2010.

Vassilev, S. V., Baxter, D., Andersen, L. K., and Vassileva, C. G.: An overview of the chemical composition of biomass, *Fuel*, 89, 913–933, doi:10.1016/j.fuel.2009.10.022, 2010.

Vestreng, V., Myhre, G., Fagerli, H., Reis, S., and Tarrasón, L.: Twenty-five years of continuous sulphur dioxide emission reduction in Europe, *Atmos. Chem. Phys.*, 7, 3663–3681, doi:10.5194/acp-7-3663-2007, 2007.

Wang, R., Tao, S., Ciais, P., Shen, H. Z., Huang, Y., Chen, H., Shen, G. F., Wang, B., Li, W., Zhang, Y. Y., Lu, Y., Zhu, D., Chen, Y. C., Liu, X. P., Wang, W. T., Wang, X. L., Liu, W. X., Li, B. G., and Piao, S. L.: High-resolution mapping of combustion processes and implications for CO₂ emissions, *Atmos. Chem. Phys.*, 13, 5189–5203, doi:10.5194/acp-13-5189-2013, 2013.

Wang, R., Tao, S., Shen, H. Z., Huang, Y., Chen, H., Balkanski, Y., Boucher, O., Ciais, P., Shen, G. F., Li, W., Zhang, Y. Y., Chen, Y. C., Lin, N., Su, S., Li, B. G., Liu, J. F., and Liu, W. X.: Trend in global black carbon emissions from 1960 to 2007, *Environ. Sci. Technol.*, 48, 6780–6787, doi:10.1021/Es5021422, 2014a.

Sources, transport and deposition of iron in the global atmosphere

R. Wang et al.

Title Page

Abstract

Introduction

Conclusions

References

Tables

Figures

◀

▶

◀

▶

Back

Close

Full Screen / Esc

Printer-friendly Version

Interactive Discussion



- Wang, R., Tao, S., Balkanski, Y., Ciais, P., Boucher, O., Liu, J. F., Piao, S. L., Shen, H. Z., Vuolo, M. R., Valari, M., Chen, H., Chen, Y. C., Cozic, A., Huang, Y., Li, B. G., Li, W., Shen, G. F., Wang, B., and Zhang, Y. Y.: Exposure to ambient black carbon derived from a unique inventory and high-resolution model, *P. Natl. Acad. Sci. USA*, 111, 2459–2463, doi:10.1073/pnas.1318763111, 2014b.
- 5 Wang, R., Balkanski, Y., Boucher, O., Ciais, P., Penuelas, J., and Tao, S.: Significant contribution of combustion-related emissions to the atmospheric phosphorus budget, *Nat. Geosci.*, 1, 48–54, 2015.
- 10 Wang, Y. F., Huang, K. L., Li, C. T., Mi, H. H., Luo, J. H., and Tsai, P. J.: Emissions of fuel metals content from a diesel vehicle engine, *Atmos. Environ.*, 37, 4637–4643, doi:10.1016/j.atmosenv.2003.07.007, 2003.
- Yen, C.: High volume fly ash concrete manufacturing technique and application study, Technical Report for the Taiwan Power Company, 275 pp., Taipei, Taiwan, 2011.
- 15 Yi, H. H., Hao, J. M., Duan, L., Tang, X. L., Ning, P., and Li, X. H.: Fine particle and trace element emissions from an anthracite coal-fired power plant equipped with a bag-house in China, *Fuel*, 87, 2050–2057, doi:10.1016/j.fuel.2007.10.009, 2008.
- Zhang, H. F., Ye, X. N., Cheng, T. T., Chen, J. M., Yang, X., Wang, L., and Zhang, R. Y.: A laboratory study of agricultural crop residue combustion in China: emission factors and emission inventory, *Atmos. Environ.*, 42, 8432–8441, doi:10.1016/j.atmosenv.2008.08.015, 2008.

Sources, transport and deposition of iron in the global atmosphere

R. Wang et al.

Title Page

Abstract

Introduction

Conclusions

References

Tables

Figures

◀

▶

◀

▶

Back

Close

Full Screen / Esc

Printer-friendly Version

Interactive Discussion



Table 1. Comparison of Fe emissions from combustion and mineral sources (Tg yr^{-1}) in the present work and previous studies. The Fe content of dust used to estimate Fe emissions from mineral sources (F_c) is given in brackets.

Study	Year(s)	Fossil fuels	Biomass burning	Mineral source
Bertine and Goldberg (1971)	1967	1.4 (all sizes)		
Luo et al. (2008)	1996	0.56 (PM_{1-10}) 0.10 (PM_1)	0.86 (PM_{1-10}) 0.21 (PM_1)	55 ($F_c = 3.5\%$)
Ito (2013)	2001	0.44 (PM_{1-10}) 0.07 (PM_1)	0.92 (PM_{1-10}) 0.23 (PM_1)	74 ($F_c = 3.5\%$)
Present study	1967	3.0 (all sizes)		
	1996	1.14 (PM_{1-10}) 0.036 (PM_1)	0.31 (PM_{1-10}) 0.012 (PM_1)	
		2001	0.83 (PM_{1-10}) 0.035 (PM_{1-10})	0.31 (PM_{1-10}) 0.012 (PM_1)
	2000–2011			38.5 ($F_c = 3.5\%$)
	2000–2011			41.0 (F_c using new mineralogical data)

Sources, transport and deposition of iron in the global atmosphere

R. Wang et al.

Table 2. Statistics for the comparison of modelled and observed Fe concentrations. N , sample size; F_2 and F_5 , fractions of stations with deviations within a factor of two or five, respectively; NMB, normalized mean bias. The values in brackets show the indicators when the combustion sources are not included.

	N	F_2 (%)	F_5 (%)	NMB (%)
Indian Ocean	61	30 (30)	75 (75)	−68 (−68)
Atlantic Ocean	224	64 (63)	82 (79)	15 (14)
Pacific Ocean	126	52 (48)	69 (67)	−66 (−69)
South Ocean	47	43 (36)	53 (43)	−48 (−79)
East Asia	32	84 (13)	100 (31)	−2 (−78)
South America	4	50 (50)	75 (50)	−78 (−91)
North America	12	83 (33)	100 (67)	−40 (−66)
Mediterranean	23	61 (57)	87 (87)	24 (16)
All regions	529	57 (49)	77 (70)	−14 (−32)

Title Page

Abstract

Introduction

Conclusions

References

Tables

Figures

◀

▶

◀

▶

Back

Close

Full Screen / Esc

Printer-friendly Version

Interactive Discussion



Sources, transport and deposition of iron in the global atmosphere

R. Wang et al.

Table 3. Global Fe budgets from various sources and from different particle size classes. The total deposition of Fe was calculated over land and oceans separately, and was also calculated for the dry deposition (DRY), wet deposition (WET), and sedimentation (SED), respectively.

	Source (Tgyr ⁻¹)	Burden (Gg)	Lifetime (days)	Deposition (Tgyr ⁻¹)		Deposition (Tgyr ⁻¹)		
				over land	over ocean	DRY	WET	SED
Coal								
PM ₁	0.018	0.262	5.28	0.013	0.005	0.008	0.010	0.0002
PM _{1–10}	1.025	6.437	2.30	0.807	0.215	0.310	0.331	0.381
PM _{>10}	3.167	0.431	0.05	2.905	0.235	0.142	0.026	2.971
Total	4.210	7.131	0.26	3.724	0.455	0.460	0.367	3.352
Petroleum								
PM ₁	0.020	0.289	5.20	0.010	0.010	0.007	0.013	0.0002
PM _{1–10}	0.002	0.014	2.22	0.001	0.001	0.001	0.001	0.001
Total	0.022	0.303	4.79	0.011	0.011	0.008	0.014	0.001
Biomass								
PM ₁	0.012	0.312	9.39	0.008	0.004	0.004	0.007	0.0002
PM _{1–10}	0.324	3.660	4.13	0.253	0.071	0.090	0.127	0.106
PM _{>10}	0.251	0.057	0.08	0.243	0.009	0.012	0.003	0.237
Total	0.587	4.030	1.27	0.503	0.083	0.101	0.130	0.343
Dust	41.0	442	3.95	33.0	7.82	15.3	15.1	10.4

Sources, transport and deposition of iron in the global atmosphere

R. Wang et al.

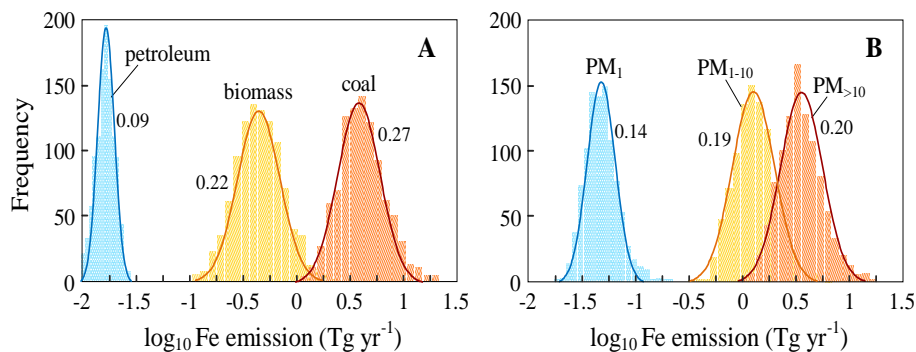


Figure 1. Frequency distributions of Fe emissions from different fuel types **(a)** and particle sizes **(b)**. The distributions are derived from 1000 Monte Carlo simulations. The standard deviation of log₁₀-transformed Fe emissions is shown for each distribution. The x axes are plotted on a log scale.

[Title Page](#)[Abstract](#)[Introduction](#)[Conclusions](#)[References](#)[Tables](#)[Figures](#)[◀](#)[▶](#)[◀](#)[▶](#)[Back](#)[Close](#)[Full Screen / Esc](#)[Printer-friendly Version](#)[Interactive Discussion](#)

Sources, transport and deposition of iron in the global atmosphere

R. Wang et al.

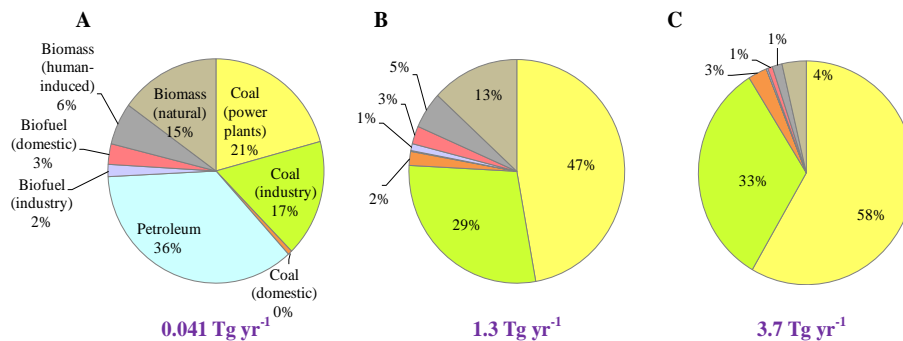


Figure 2. Source profiles of Fe from combustion for PM₁ (a), PM_{1–10} (b), and PM_{>10} (c) as an average for 1960–2007. The total Fe emission for each size class is provided under its pie chart.

Sources, transport and deposition of iron in the global atmosphere

R. Wang et al.

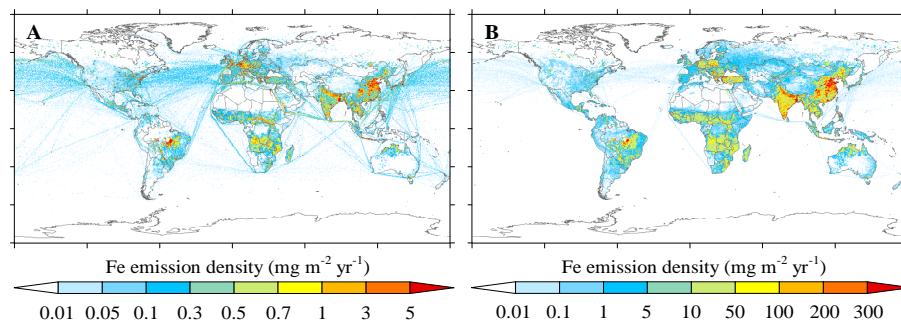


Figure 3. Spatial distributions of Fe emissions from combustion sources in 2007 at a resolution of $0.1^\circ \times 0.1^\circ$ for fine (PM₁) (a) and medium-to-coarse (PM₁₋₁₀ and PM_{>10}) (b) particles.

[Title Page](#)[Abstract](#)[Introduction](#)[Conclusions](#)[References](#)[Tables](#)[Figures](#)[◀](#)[▶](#)[◀](#)[▶](#)[Back](#)[Close](#)[Full Screen / Esc](#)[Printer-friendly Version](#)[Interactive Discussion](#)

Sources, transport and deposition of iron in the global atmosphere

R. Wang et al.

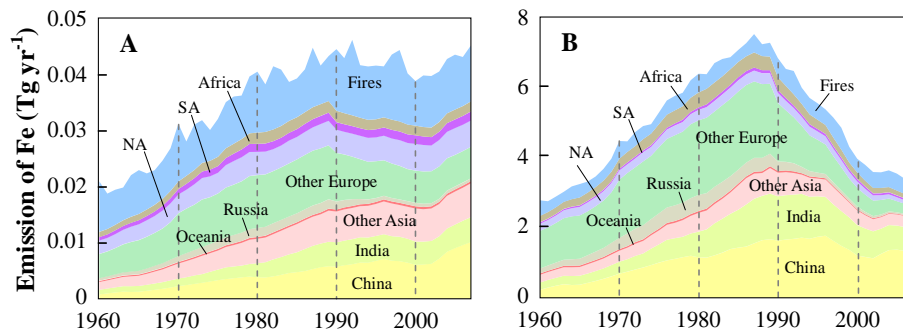


Figure 4. Temporal trends of Fe emissions of fine (PM_{1}) (a) and medium-to-coarse (PM_{1-10} and $PM_{>10}$) (b) particles from combustion sources from 1960 to 2007. Fe emissions from wildfires are shown separately with energy-related activities separated by region (NA for North America and SA for South America).

Title Page

Abstract

Introduction

Conclusions

References

Tables

Figures

◀

▶

◀

▶

Back

Close

Full Screen / Esc

Printer-friendly Version

Interactive Discussion



Sources, transport and deposition of iron in the global atmosphere

R. Wang et al.

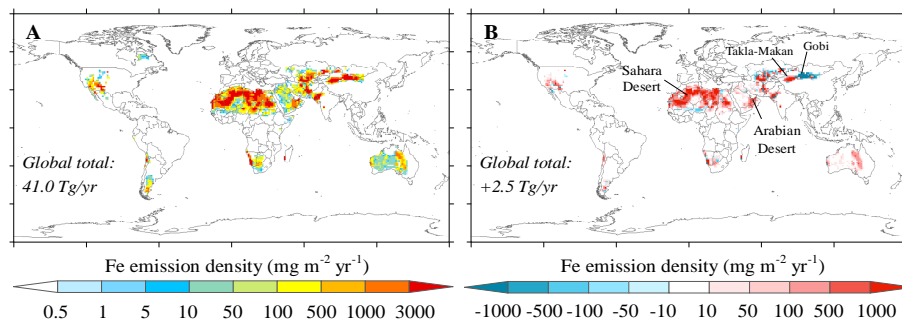


Figure 5. Average Fe emission from dust sources for 2000–2011 using the new mineralogical data set **(a)** and the difference of average Fe emission from dust sources for 2000–2011 using the new mineralogical data set relative to that using a constant Fe content (3.5%) **(b)**. A positive value in **(b)** indicates a larger emission density by using the new mineralogical data set.

Title Page

Abstract

Introduction

Conclusions

References

Tables

Figures

◀

▶

◀

▶

Back

Close

Full Screen / Esc

Printer-friendly Version

Interactive Discussion



Sources, transport and deposition of iron in the global atmosphere

R. Wang et al.

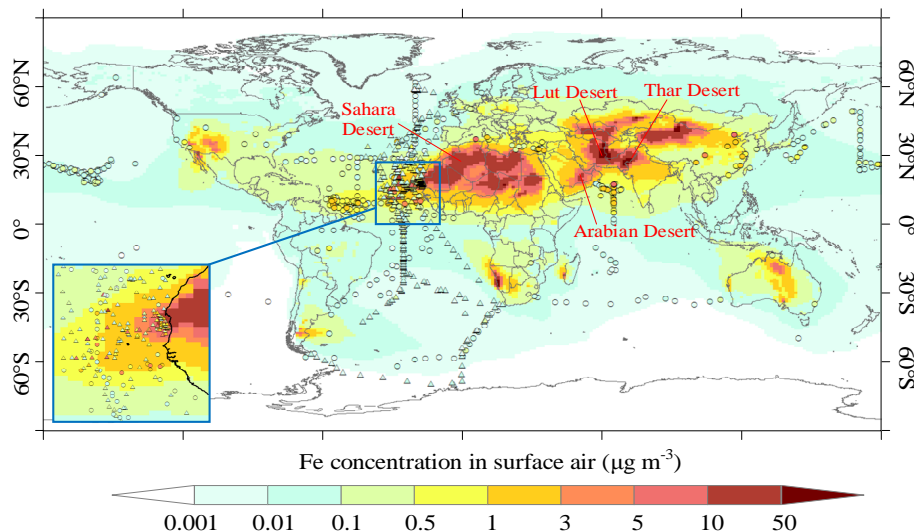


Figure 6. Distribution of annual mean concentrations of Fe attached to aerosols in surface air. A total of 529 measured Fe concentrations compiled by Mahowald et al. (2009) and Sholkovitz et al. (2012) and collected in this study (Table S3) are shown as circles, and a total of 296 Fe concentrations measured by Baker et al. (2013) over the Atlantic Ocean are shown as triangles.

[Title Page](#)[Abstract](#)[Introduction](#)[Conclusions](#)[References](#)[Tables](#)[Figures](#)[◀](#)[▶](#)[◀](#)[▶](#)[Back](#)[Close](#)[Full Screen / Esc](#)[Printer-friendly Version](#)[Interactive Discussion](#)

Sources, transport and deposition of iron in the global atmosphere

R. Wang et al.

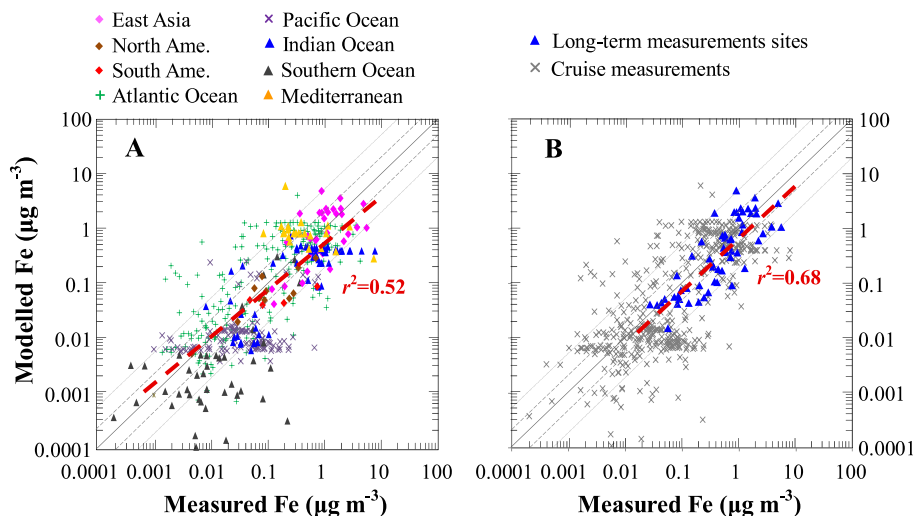


Figure 7. Comparisons of modelled and observed Fe concentrations by region **(a)** and measuring type **(b)**. The modelled concentrations are averaged for the months in the year of measurements. The fitted curves for all stations in **(a)** and long-term measurement stations in **(b)** are shown as red dashed lines, with coefficients of determination (r^2) listed. The 1 : 1 (solid), 1 : 2 and 2 : 1 (dashed), and 1 : 5 and 5 : 1 (dotted) lines are shown.

Title Page

Abstract

Introduction

Conclusions

References

Tables

Figures

◀

▶

◀

▶

Back

Close

Full Screen / Esc

Printer-friendly Version

Interactive Discussion

Sources, transport and deposition of iron in the global atmosphere

R. Wang et al.

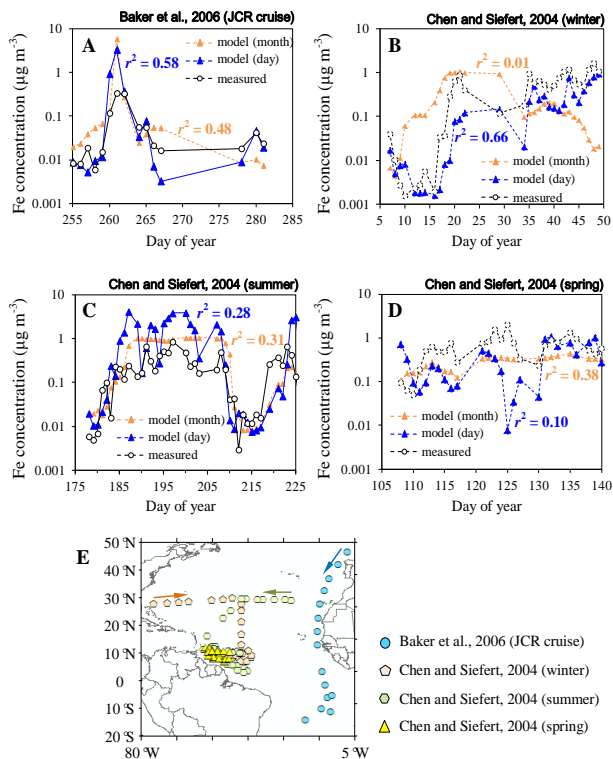


Figure 8. Comparisons of modelled and measured Fe concentrations. The Fe concentrations were derived as monthly (blue triangles) or daily (orange triangles) means from the model. **(a)** Fe measured in autumn 2001 (James Clark Ross (JCR) cruise) by Baker et al. (2006). **(b)** Fe measured in winter 2001 by Chen and Siefert (2004). **(c)** Fe measured in summer 2001 by Chen and Siefert (2004). **(d)** Fe measured in spring 2003 by Chen and Siefert (2004). **(e)** Locations of the cruise measurements **(a–d)**.

Title Page

Abstract

Introduction

Conclusions

References

Tables

Figures

◀

▶

◀

▶

Back

Close

Full Screen / Esc

Printer-friendly Version

Interactive Discussion

Sources, transport and deposition of iron in the global atmosphere

R. Wang et al.

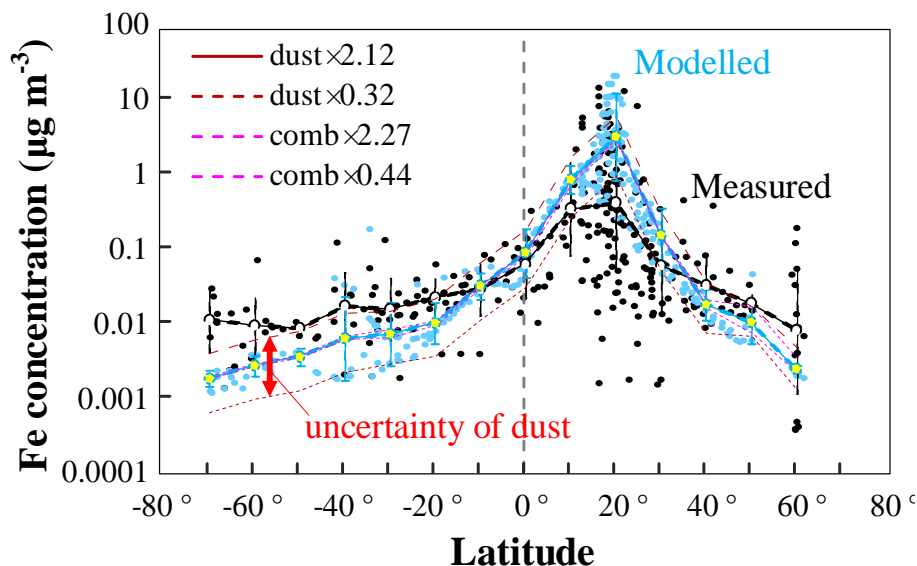


Figure 9. Zonal distribution of modelled (blue dots) and measured (black dots) Fe concentrations attached to aerosols in surface air over the Atlantic Ocean from 70° S to 60° N. The blue and black lines show the modelled and measured Fe concentrations as geometric means in each band with error bars for the geometric standard deviations. As sensitivity tests, Fe concentrations from mineral sources were scaled by factors of 0.32 and 2.12 as 90 % uncertainties in dust emissions (Huneeus et al., 2011) and Fe concentrations from combustion sources were scaled by factors of 0.44 and 2.27 as 90 % uncertainties in Fe emissions from combustion.

Title Page

Abstract

Introduction

Conclusions

References

Tables

Figures

◀

▶

◀

▶

Back

Close

Full Screen / Esc

Printer-friendly Version

Interactive Discussion



Sources, transport and deposition of iron in the global atmosphere

R. Wang et al.

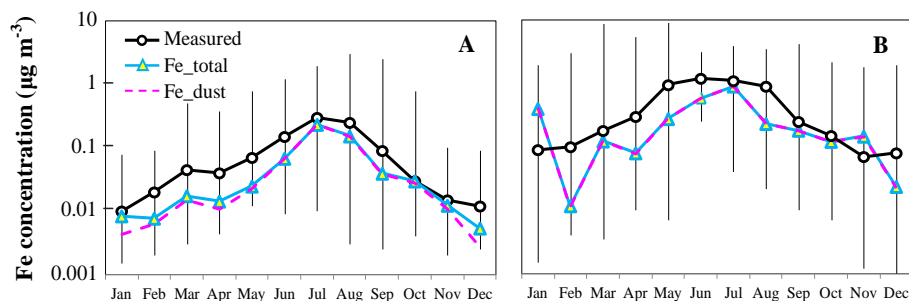


Figure 10. Seasonality of Fe concentrations attached to aerosols in surface air at Bermuda (32.2° N , 64.5° W) (a) and Barbados (13.2° N , 59.3° W) (b) on the western margin of the Atlantic Ocean. Modelled Fe concentrations are derived from all sources (Fe_{total}) and from mineral sources only (Fe_{dust}). Measured Fe concentrations are shown as the medians (circles) for 1988–1994 with the ranges between the 10th and 90th percentiles (error bars).

Sources, transport and deposition of iron in the global atmosphere

R. Wang et al.

Title Page

Abstract

Introduction

Conclusions

References

Tables

Figures



Back

Close

Full Screen / Esc

Printer-friendly Version

Interactive Discussion

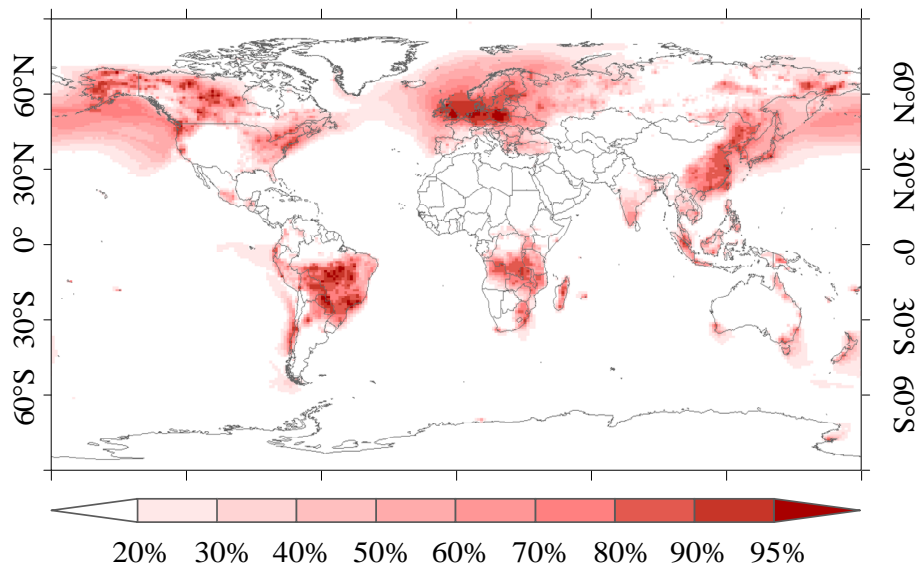


Figure 11. Relative contribution of combustion sources to the modelled Fe concentrations attached to aerosols in surface air.

Sources, transport and deposition of iron in the global atmosphere

R. Wang et al.

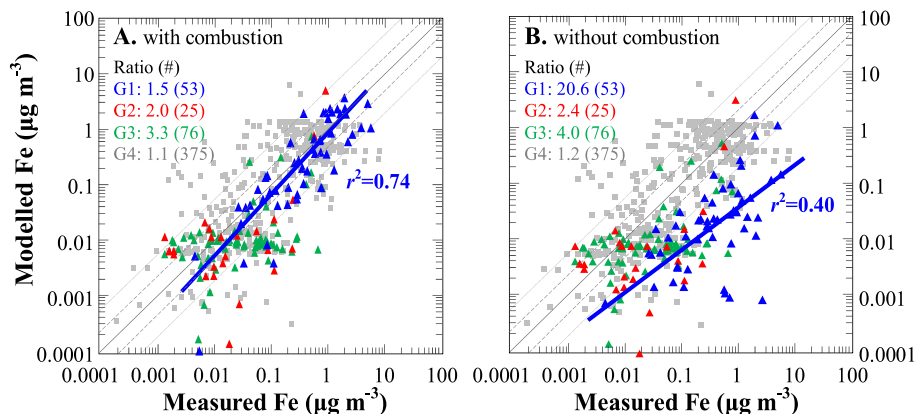


Figure 12. Plots of modelled and measured Fe concentrations attached to aerosols in surface air with (a) or without (b) combustion sources. All stations were divided into four groups based on the contribution of combustion sources: G1, contribution $\geq 50\%$ (blue triangles); G2, $30\% \leq$ contribution $< 50\%$ (red triangles); G3: $15\% \leq$ contribution $< 30\%$ (green triangles); G4, contribution $< 15\%$ (grey squares). The ratios between measured and modelled concentrations as geometric means are listed with the number of stations in the brackets for each group. The fitted curves for the G1 stations are shown as blue lines with coefficients of determination (r^2).

[Title Page](#)
[Abstract](#)
[Introduction](#)
[Conclusions](#)
[References](#)
[Tables](#)
[Figures](#)
[◀](#)
[▶](#)
[◀](#)
[▶](#)
[Back](#)
[Close](#)
[Full Screen / Esc](#)
[Printer-friendly Version](#)
[Interactive Discussion](#)


Sources, transport and deposition of iron in the global atmosphere

R. Wang et al.

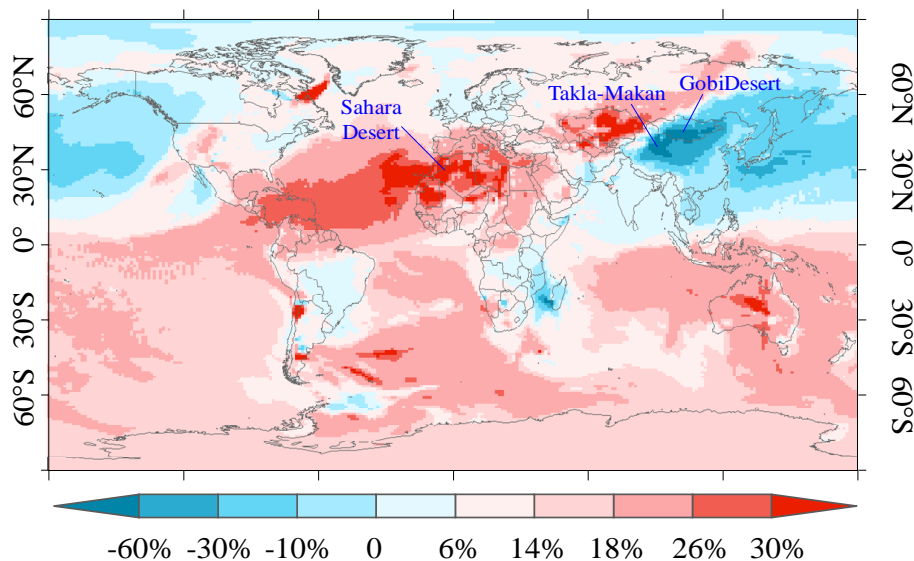


Figure 13. Relative differences in simulated Fe concentrations attached to aerosols in surface air when using the new mineralogical data and prescribing a constant Fe content in dust (3.5%). A positive difference indicates a higher Fe concentration when using the new mineralogical data.

Title Page

Abstract

Introduction

Conclusions

References

Tables

Figures



Back

Close

Full Screen / Esc

Printer-friendly Version

Interactive Discussion



Sources, transport and deposition of iron in the global atmosphere

R. Wang et al.

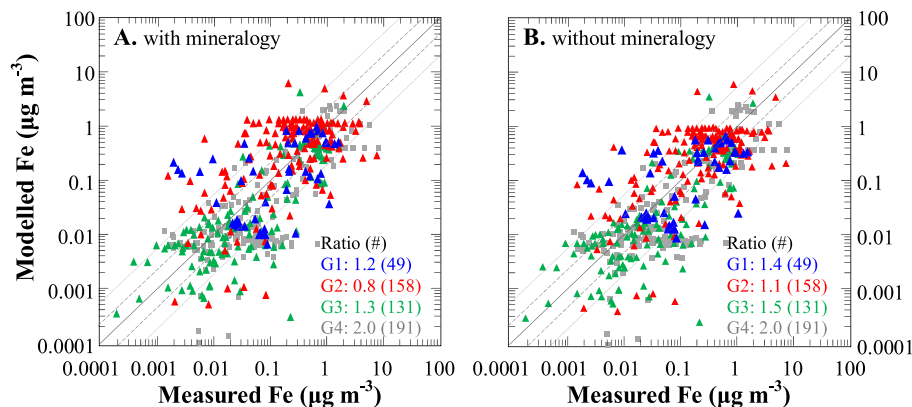


Figure 14. Plots of modelled and measured Fe concentrations attached to aerosols in surface air. The Fe content of dust was calculated from the new mineralogical data **(a)** or prescribed as 3.5 % **(b)**. All stations were divided into four groups based on the relative differences between **(a)** and **(b)**: G1, difference $\geq 30\%$ (blue triangles); G2, $20\% \leq$ difference $< 30\%$ (red triangles); G3, $10\% \leq$ difference $< 20\%$ (green triangles); G4, difference $< 10\%$ (grey squares). The ratios between measured and modelled concentrations as geometric means are listed with the number of stations in brackets for each group.

Title Page

Abstract

Introduction

Conclusions

References

Tables

Figures



Back

Close

Full Screen / Esc

Printer-friendly Version

Interactive Discussion



Sources, transport and deposition of iron in the global atmosphere

R. Wang et al.

Title Page

Abstract

Introduction

Conclusions

References

Tables

Figures



Back

Close

Full Screen / Esc

Printer-friendly Version

Interactive Discussion

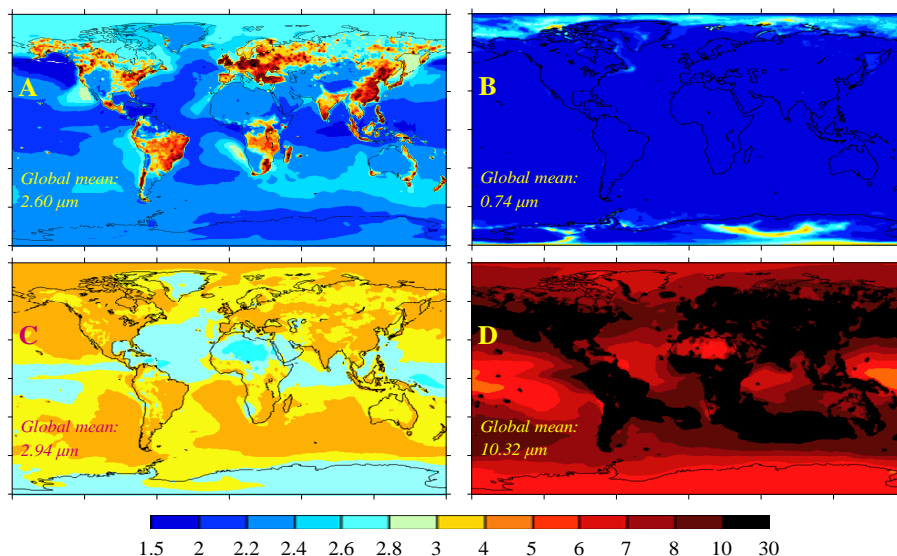


Figure 15. Spatial distributions of the wet mass median diameter (μm) of Fe-containing particles in surface air. **(a)** Fe from all combustion and mineral sources. **(b–d)** Fe from coal combustion in PM_1 **(b)**, PM_{1-10} **(c)**, and $\text{PM}_{>10}$ **(d)**. The global mean is provided in each panel.

Sources, transport and deposition of iron in the global atmosphere

R. Wang et al.

Title Page

Abstract

Introduction

Conclusions

References

Tables

Figures



Back

Close

Full Screen / Esc

Printer-friendly Version

Interactive Discussion

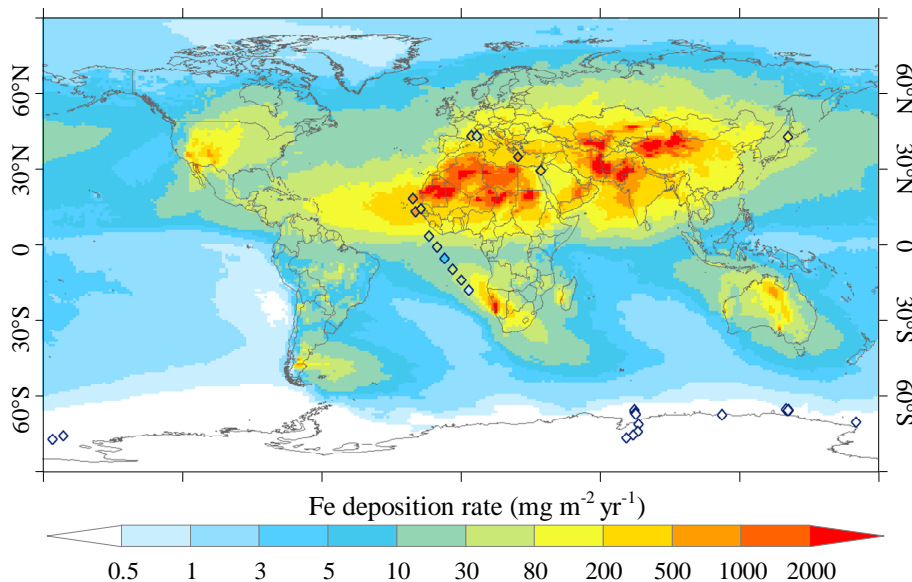


Figure 16. Global distribution of modelled annual mean Fe deposition rates. The observed Fe deposition rates from in situ measurements compiled by Mahowald et al. (2009) are shown as diamonds of the same color as the scale.

Sources, transport and deposition of iron in the global atmosphere

R. Wang et al.

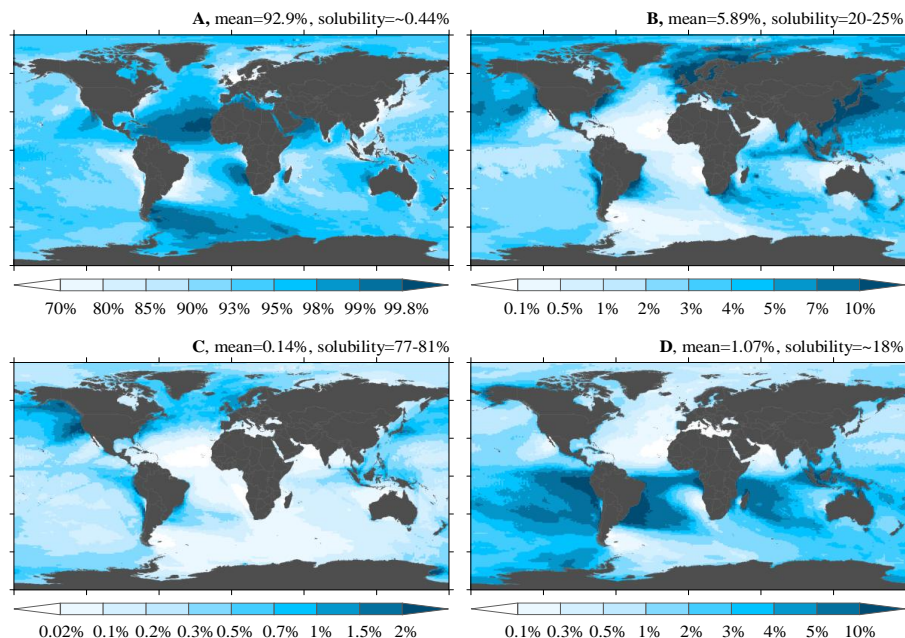


Figure 17. Relative contributions of atmospheric Fe deposition over oceans by mineral sources (a) and combustion of coal (b), oil (c), and biomass (d). The average contribution over the oceans and the measured Fe solubility are provided in the panel descriptions. Color scales differ on each plot.

Title Page

Abstract

Introduction

Conclusions

References

Tables

Figures

◀

▶

◀

▶

Back

Close

Full Screen / Esc

Printer-friendly Version

Interactive Discussion



Sources, transport and deposition of iron in the global atmosphere

R. Wang et al.

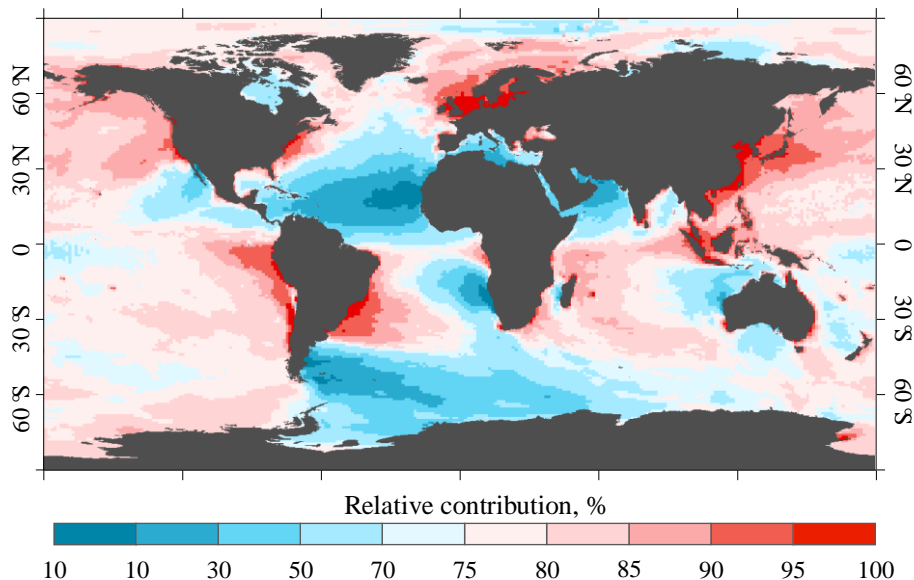


Figure 18. Relative contribution of combustion-related emissions to atmospheric soluble Fe deposition over oceans. Constant Fe solubilities (0.44 % for dust, 22.5 % for coal fly ash, 79 % for oil fly ash and 18 % for biomass fly ash) were applied to calculate the deposition of soluble Fe from the deposition of total Fe.

[Title Page](#)[Abstract](#)[Introduction](#)[Conclusions](#)[References](#)[Tables](#)[Figures](#)[◀](#)[▶](#)[◀](#)[▶](#)[Back](#)[Close](#)[Full Screen / Esc](#)[Printer-friendly Version](#)[Interactive Discussion](#)